HHS Public Access

Author manuscript

JACC Cardiovasc Imaging. Author manuscript; available in PMC 2016 March 01.

Published in final edited form as:

JACC Cardiovasc Imaging. 2015 March ; 8(3): 288–318. doi:10.1016/j.jcmg.2014.12.013.

Echocardiographic Imaging of Procedural Complications During Balloon-Expandable Transcatheter Aortic Valve Replacement

Rebecca T. Hahn, MD[*], **Susheel Kodali, MD**[*], **E. Murat Tuzcu, MD**[†], **Martin B. Leon, MD**[*], **Samir Kapadia, MD**[†], **Deepika Gopal, MD**[‡], **Stamatios Lerakis, MD**[§], **Brian R. Lindman, MD**[‖], **Zuyue Wang, MD**[¶], **John Webb, MD**[#], **Vinod H. Thourani, MD**[§], and **Pamela S. Douglas, MD**[**]

[*]the Columbia University Medical Center/New York-Presbyterian Hospital, New York, New York

[†]Cleveland Clinic Foundation, Cleveland, Ohio

[‡]Baylor Scott & White Health, Plano, Texas

[§]Emory University School of Medicine, Atlanta, Georgia

[‖]Washington University School of Medicine, St. Louis, Missouri

[¶]Medstar Health Research Institute, Washington, DC

[#]University of British Columbia and St. Paul's Hospital, Vancouver, Ontario, Canada

[**]Division of Cardiovascular Medicine, Duke University Medical Center, and Duke Clinical Research Institute, Durham, North Carolina

Abstract

Transcatheter aortic valve replacement (TAVR) using a balloon-expandable valve is an accepted alternative to surgical replacement for severe, symptomatic aortic stenosis in high risk or inoperable patients. Intraprocedural transesophageal echocardiography (TEE) offers real-time imaging guidance throughout the procedure and allows for rapid and accurate assessment of complications and procedural results. The value of intraprocedural TEE for TAVR will likely increase in the future as this procedure is performed in lower surgical risk patients, who also have lower risk for general anesthesia, but a greater expectation of optimal results with lower morbidity and mortality. This imaging compendium from the PARTNER (Placement of Aortic Transcatheter Valves) trials is intended to be a comprehensive compilation of intraprocedural complications imaged by intraprocedural TEE and diagnostic tools to anticipate and/or prevent their occurrence.

Keywords

aortic stenosis; echocardiography; transcatheter aortic valve replacement

Reprint Requests and Correspondence: Dr. Rebecca T. Hahn, Columbia University Medical Center, New York-Presbyterian Hospital, 177 Fort Washington Avenue, New York, New York 10032. rth2@columbia.edu.

Appendix For supplemental videos, please see the online version of this article.

Transcatheter aortic valve replacement (TAVR) using a balloon-expandable valve is an accepted alternative to surgical replacement for severe, symptomatic aortic stenosis in high-risk or inoperable patients (1,2). Although echocardiography is important in the pre-procedural evaluation of patients undergoing TAVR (particularly to characterize and quantitate the severity of aortic stenosis [3,4] and assist in valve sizing [5,6]), other imaging modalities (e.g., computed tomography) are also useful for assessing the aortic valvular complex before transcatheter heart valve (THV) implantation (7–18). However, intraprocedural transesophageal echocardiography (TEE) offers the significant advantage of accurate real-time imaging and is incomparable in its ability to anticipate procedural complications and verify procedural results (19–21). Moreover, intraoperative TEE provides rapid and accurate information for detection of potentially lethal complications. Prompt diagnosis and subsequent treatment improve outcomes (21). Although some centers choose not to use this imaging tool during TAVR (22), other sites have advocated using TEE as the primary imaging tool (23), reporting a significant reduction in contrast media use with no reduction in safety.

The value of intraprocedural TEE is unlikely to diminish in the future. Current guidelines continue to advocate the use of TEE as a critically important component of the intraprocedural and immediate post-procedural success of TAVR (19,24,25). Recent studies suggesting that intraprocedural TEE may not be necessary for TAVR (22,26–29) fail to appreciate that the safety bar will be even higher in moderate risk patients who are subjected to TAVR. Sites using the “minimalist approach” are highly experienced, and recommending this approach to implant operators with lower procedural volumes may be ill advised. In fact, in a study of an intermediate risk population using the minimalist approach (26) the 30 day mortality rate is in fact higher than that reported in a higher risk patient population of the PARTNER (Placement of Aortic Transcatheter Valves) trial (30).

Because TAVR is a relatively new procedure, it is important for both experienced and novice operators to be aware of the echocardiographic appearance of major complications and for the interventionalists to react to those findings. There have been multiple reports of complications of the procedure, including access issues (31–33), aortic root trauma (34–36), malpositioning of the THV (37–39), coronary obstruction (40,41), paravalvular regurgitation (PAR) (42–49), ventricular septal or mitral leaflet perforation (35), and cardiogenic shock (50,51). This imaging compendium from the PARTNER trials is intended to be a comprehensive compilation of intraprocedural complications imaged by using intraprocedural TEE and diagnostic tools to anticipate and/or prevent their occurrence. The compendium uses both standard and structure-specific imaging planes outlined in the recent American Society of Echocardiography (ASE) guidelines (25) as well as the guidelines for 3-dimensional (3D) echocardiographic imaging acquisition and display (52). Imaging planes and transducer angles are well described in the guidelines and will not be included in this paper.

The intended audience for this report includes experienced and beginning “procedural” echocardiographers, as well as interventionalists and surgeons performing TAVR. It is intended to serve both as a teaching guide providing “tips and tricks” to assist in daily practice and as a reference work containing unusual or exceptional findings. Because the

PARTNER trials represent the initial experience with TAVR in the United States, many of the findings indicate steps on the learning curve for the field as well as for each of the participating research sites, almost none of whom had experience with this procedure. Documenting these early missteps is highly informative even though some of these findings may rarely occur for current, more experienced teams.

A total of 527 patients in the PARTNER 1 trial underwent TAVR with the first generation balloon-expandable THV (Edwards SAPIEN, Edwards Lifesciences, Irvine, California). The list of complications in Table 1 was compiled by reviewing the adverse event log from the PARTNER I trial and the core laboratory records for complications noted on transthoracic echocardiographic follow-up. Complications that could be imaged by intraprocedural echocardiography were determined and sites polled for the availability of the original TEE images. Images were collected and reviewed. Of note, all the complications on the list had associated images, which are presented here. Important imaging considerations are summarized in Table 2.

Complications

Stiff Wire Location

Complications can occur during extra-stiff wire positioning. The most common complication is entanglement in the mitral apparatus. This is frequently recognized by paying strict attention to any change in mitral valve morphology or severity of regurgitation (Figure 1A, Online Video 1). 3D imaging may help confirm the site of entanglement (Figure 1B). When recognized, repositioning the wire may avoid other complications, such as rupture of mitral chordal attachments with subsequent flail leaflet (Figures 1C and 1D). The wire may also perforate the septum during transapical procedures, causing a ventricular septal defect.

Balloon aortic valvuloplasty complications

For the balloon-expandable valve, most operators use a balloon aortic valvuloplasty (BAV) to increase valve opening and improve precise positioning of the THV. Some investigators use the stability of the balloon catheter during BAV as a possible predictor of operator-independent motion of the THV and subsequent malpositioning. BAV is also used as adjunctive imaging for THV sizing (53–55) and to predict the final position of the native cusps after TAVR. Although complications with BAV are rare, they vary in appearance and many can be imaged during the procedure (e.g., severe aortic regurgitation, pericardial effusion) by using intraprocedural TEE (56).

Immediately after BAV, it is important to assure the interventionalists that the valve remains intact and that the aortic regurgitation is not significantly increased. In the first case (Figures 2A and 2B, Online Video 2), the etiology of the regurgitation is an avulsed aortic valve (AV). In the second case (Figures 2C and 2D, Online Video 3), the etiology is a displaced and fixed left coronary cusp. The latter complication may resolve spontaneously if the cusps quickly resume their “closed” position; however, because of the acute hemodynamic compromise that frequently occurs with torrential acute aortic regurgitation, immediate deployment of the THV is usually indicated.

BAV can also be used as a diagnostic test to anticipate possible complications. Rupture of the balloon during BAV is typically caused by spicules of calcium. If rupture of the balloon occurs during deployment of the THV, the valve may be significantly underdeployed, which increases the risk of acute THV embolization. Continuous imaging during BAV may also predict the final location of the bulky calcified cusps in relation to the aortic root wall as well as the left main coronary artery. In the setting of small sinuses of Valsalva, bulky calcified cusps may threaten the integrity of the aortic root, and deformation of the root can be imaged during BAV (Figure 3A, Online Video 4) and help predict subsequent trauma to the aorta with TAVR, such as a periaortic hematoma (Figure 3B, Online Video 5). Coronary occlusion has been associated with female sex, small aortic root (sinus diameter 27.8 ± 2.0 mm), and height of the left main coronary above the annulus. Because no obstructions appear to be related to THV strut obstruction, the likely mechanism is direct obstruction by the calcified left coronary cusp (41). Intraprocedural measurement of the left main coronary height (above the annulus) and length of the left coronary cusp using 3D echocardiography (Figures 4A and 4B) alerts the interventionalists to the possibility of left main coronary artery occlusion by a bulky, calcified left coronary cusp. Once a discordance between coronary height and cusp length is detected (with cusp length typically >2 mm longer than the coronary height), the diameter of the relevant sinus of Valsalva is then measured. If this diameter is ≤30 mm, the risk for occlusion is significant, and intraprocedural imaging during BAV can then be used as a diagnostic test allowing direct visualization of the orifice of the left main coronary artery with maximum balloon inflation (Figure 5, Online Video 6). In the example shown, bulky calcium filled the left main ostium, and a crimped coronary stent was adjunctively positioned in the left main coronary artery before TAVR. After valve deployment, there was nearly complete occlusion of the left main, and the coronary stent was quickly deployed.

Acute hemodynamic compromise

In the setting of hemodynamic collapse, the prompt and accurate diagnosis of the underlying problem has paramount importance. While the anesthesiologist is managing the hemodynamics and the ventilator, the etiology of the acute hypotension must be rapidly diagnosed by using intraprocedural TEE (25). Rapid assessment of valvular (mitral, THV, tricuspid, and pulmonic) morphology/function, aortic pathology, coronary patency, biventricular function, root rupture, and pericardial effusion can be performed within minutes. Hypovolemia and bleeding can be suggested by comparing ventricular size with baseline imaging. Ruling out such causes is invaluable for the treatment of these potentially lethal complications.

Rapid pacing is used to reduce forward flow during both BAV and TAVR. In those patients (typically with significantly reduced baseline left or right ventricular function), the 5 to 10 s of low forward flow may cause significant global or regional ischemia, resulting in severe persistent hypotension or even cardiac arrest/pulseless electrical activity (Figure 6). Allowing these patients to recover their blood pressure and ventricular function between BAV and TAVR may avoid significant hemodynamic compromise.

Malposition and failure to implant

Marked and typically focal hypertrophy of the basal septum is not uncommon in elderly subjects with severe aortic stenosis. In the setting of marked hypertrophy as well as dynamic narrowing of the left ventricular outflow tract (LVOT), there are a number of risks, primarily related to accurate placement of the balloon-expandable valve. This dynamic narrowing can be best appreciated by using 3D TEE (Figure 7, Online Video 7). Operator-independent motion of the valve prosthesis (either ventricular or aortic) due to marked dynamic narrowing of the LVOT can result in significant malposition of the valve (Figure 8, Online Video 8). There are no strict criteria for septal thickness or degree of LVOT narrowing that would warrant aborting the procedure; however, the BAV may again be helpful in the decision-making process. One patient in the current study had severe septal hypertrophy that pushed the BAV balloon into the ascending aorta on repeated valvuloplasties; this increased the concern of malpositioning, which prompted the interventionalist to abort the procedure.

A large meta-analysis of 9,251 patients from 46 studies reported a low rate of bailout surgery (1.1 ± 1.1%); the most frequently reported reason for emergent surgery was embolization/dislocation of the AV prosthesis (41%) (57). Malpositioning of the valve is also recognized as an important factor contributing to the presence of paravalvular aortic regurgitation (PAR) as well as poor THV hemodynamics, mitral valve compromise, and conduction defects (35,58–66).

Accurate positioning of the balloon-expandable valve requires an understanding of the motion and shortening of the THV during deployment. Fluoroscopy has shown that the device-center upper movement during final deployment was (on average) 2.0 ± 1.43 mm (range -1.3 to 4.6 mm), with shortening of the device due to asymmetrical upward movement of the ventricular edge of THV by 3.2 ± 1.4 mm and the upper (aortic) edge by only 0.75 ± 1.50 mm (67). The optimal final THV deployment position resulted in 17% of the THV below the base of the aortic sinuses (determined by pigtail catheter position or aortography); this translated to 33% of the valve below the sinuses during the final pacing run. Multivariate analysis revealed that greater upward movement was seen with moderate and severe (vs. mild) AV calcification and smaller aortic sinus volume. Valve design iteration (first generation balloon-expandable or second generation balloon-expandable valve), procedural access (transfemoral vs. transapical), and interventricular septum width did not affect THV movement. Similar motion and shortening can be seen with echocardiography; however, the valve is positioned not by the lowest border of the sinus of Valsalva but rather by the hinge-point of the aortic cusps (i.e., the virtual annulus), which may be slightly “aortic” to the fluoroscopic landmark (Figure 9A). Because the valve typically moves up (aortic) during the pacing run, mimicking the “systolic” position during nonpaced beats, this nonpaced, diastolic valve position should be ∼50% below the hinge-point of the aortic cusps (Figure 9B). Because the ideal position of the valve is 2 to 3 mm below the annulus and the shortening of the second generation balloon-expandable valve is 3 mm primarily from the ventricular side, the valve should be typically 30% to 40% (∼5 to 6 mm) below the echocardiographic annulus during the final pacing run (Figure 9C, Online Video 9). The final position of the optimally deployed valve is ∼10% to 20% (∼2 to 3 mm)

below the hinge-points of the aortic cusps (Figure 9D). In addition to positioning according to the ventricular edge of the crimped THV, assessing the superior or aortic edge of the stented valve should be performed; the native calcified cusps must be covered by 1 to 2 mm (given the ∼1 mm shortening of the valve from this end and despite the minimal superior [aortic] motion of the THV), while remaining inferior to the sinotubular junction.

With transapical or transaortic deployment, the operator can reposition the valve during this final critical stage in a controlled, predictable way (Figure 10A). However, for transfemoral deployment, precise controlled movements remain more difficult, which can risk malpositioning. Loss of pacing capture during final deployment may also result in significant superior motion of the valve into the aorta in the setting of active ventricular contraction (Figure 10B). Positioning too low in the ventricle (Figure 10C) risks leaving leaflets uncovered or creating leaflet overhang, leading to significant central aortic regurgitation. Although a small amount of native leaflet overhang is not uncommon (particularly near the commissures where the leaflet attaches to the sinotubular junction), leaving a significant amount of calcified, rigid leaflet above the THV (Figure 11A, Online Video 10) may lead to complications. Because the calcified leaflets are the primary means of anchoring the THV, if the THV has been implanted too low with significant leaflet overhang, there can be acute (68,69) or delayed (70–72) migration of the valve into the ventricle. In theory, the calcified overhanging leaflets may exert continued downward force on the THV, thus contributing to the proximal migration. Leaflet overhang can also contribute to valve dysfunction or early valve degeneration. The use of the intraprocedural TEE is instrumental in the diagnosis of native aortic overhang. The example shown (Figure 11B, Online Video 11) reflects acute THV leaflet entrapment, resulting in significant aortic regurgitation.

Aortic complications

A number of aortic complications can occur as a result of the TAVR procedure, including aortic dissections, thoracic aorta perforation with resulting hemorrhage, and aortic annular rupture.

Aortic Dissection—Proximal aortic dissection may occur immediately (intraprocedural) or become evident later. The postulated etiology is trauma from the procedure itself (i.e., balloon dilation, the introducing catheter, deployment of the THV) or from displacement of sharp, bulky calcium during the procedure. Some dissections may be treated conservatively; however, if an acute dissection extends proximal into the sinuses of Valsalva, surgical intervention may then be necessary (particularly if the coronary arteries are threatened). An acute, intra-procedural proximal dissection is shown in Figure 12 (Online Video 12). This complication can lead to acute tamponade necessitating open repair but often with a poor outcome. Some dissections may be undiagnosed at the time of implantation, suggesting a more benign complication. Figure 13 (Online Video 13) is an example of a proximal aortic dissection diagnosed late (>6 months) after TAVR. The dissection flap extended to the sinotubular junction but not into the sinuses, and the patient was treated conservatively.

Aortic Annular Rupture—A recent multicenter retrospective study (73) studied 31 patients with aortic root rupture (20 with annular rupture and 11 with periaortic hematoma) and compared them with 31 matched control subjects. Patients with aortic root rupture had a higher degree of subannular/LVOT calcification quantified by an Agatston score of 181.2 ± 211.0 versus 22.5 ± 37.6 ($p < 0.001$), a higher frequency of ≥20% annular area oversizing (79.4% vs. 29.0%; $p < 0.001$), and an increased need for balloon post-dilation (22.6% vs. 0.0%; $p = 0.005$). In conditional logistic regression analysis for the matched data, moderate/severe LVOT/subannular calcifications (odds ratio: 10.92 [95% confidence interval: 3.23 to 36.91]; $p < 0.001$) and prosthesis oversizing ≥20% (odds ratio: 8.38 [95% confidence interval: 2.67 to 26.33]; $p < 0.001$) were associated with aortic root contained/noncontained rupture.

TEE imaging can be a valuable tool for evaluating the extent and location of LVOT calcium. This information is important in estimating the risk for annular rupture, as well as residual PAR (Figure 14, Online Videos 14 and 15). Simultaneous multiplane imaging allows an accurate assessment of the location of the calcium, which has been shown to be a predictor of PAR secondary to malapposition of the THV skirt. A risk/benefit analysis should be performed when assessing the possible effectiveness of re-ballooning to treat PAR because a small leak adjacent to a rigid calcium nodule may not resolve by using this intraprocedural therapy. Severe dystrophic calcification extending typically from the left coronary cusp into the LVOT will be forced through the annulus/adjacent myocardium during balloon inflation (Figure 15A). The resultant periaortic hematoma (Figure 15B, Online Video 16) and rapidly accumulating pericardial effusion (Figure 15C), as well as the atypical flow originating from the annulus (Figure 15D, Online Video 17), should immediately indicate the diagnosis of annular rupture. In addition to treatment of tamponade with pericardial drainage, rapid initiation of cardiopulmonary bypass should be considered.

Periaortic and Intramural Hematoma—Microrupture of the aorta resulting in periaortic hematoma deserves special mention. This complication with a reported single-site incidence of 1.6% can be managed medically if recognized early (34). In contradistinction to intramural hematoma (which is bleeding into the wall of the aorta), periaortic hematoma arises from a microperforation of all 3 layers of the aorta, and the hematoma that forms appears as a tissue-density mass around the outside of the aortic root (Figures 16A and 16B). The perforation likely occurs after stretching of the aortic wall from displaced bulky calcium during balloon inflation/deployment of the THV. This process appears to be self-limiting, with the microperforation sealing quickly once the balloon is deflated or the aorta is no longer stretched. Conservative management of the periaortic hematoma (including administration of protamine, continued intubation with restricted activity, and meticulous blood pressure control) result in excellent outcomes. Failure to recognize this complication, however, may result in uncontrolled hypertension, leading to continued bleeding within the wall of the aorta and resulting in an intramural hematoma (Figure 17). Although the outcomes in patients with TAVR are unknown, intramural hematomas in the ascending aorta have been associated with mortality rates as high as 40% when treated medically (74).

Aortic Regurgitation

It is important to distinguish between post-TAVR PAR and central aortic regurgitation since the approach to treatment of these 2 entities are different.

Paravalvular Aortic Regurgitation—Numerous studies have shown an association between post-procedural PAR and increased late mortality (30,47,49,75–80), generating intense interest in determining the factors that predict the occurrence of PAR. A recent meta-analysis confirms the importance of 3 factors: undersizing of the annulus, severity of aortic calcification, and implantation depth (49).

Determining the severity and etiology of PAR is a primary focus of post-TAVR imaging. The extent of calcification and asymmetric distribution, as well as the location of calcium on the aortic wall, valve commissure, or THV landing zone, have all been implicated as etiologies of PAR (44,47,81–86). The location and severity of calcification within the LVOT should be ascertained before TAVR; if the severity is less than mild, PAR is usually localized to regions in which calcium may prevent stent frame apposition (Figure 14). If there is a significant risk of rupture or the risk of central regurgitation from overexpansion is high, then no further intervention may be warranted. If the severity of PAR is greater than mild in the setting of a low-risk “landing zone” (i.e., no bulky calcium in the LVOT or annulus), intervention with either a post-dilation or a valve-in-valve procedure may then be warranted.

Determining the severity of PAR and thus the appropriate intraprocedural treatment remains challenging for numerous reasons. First, the ASE has suggested numerous qualitative and semi-quantitative parameters for assessing surgical prosthetic PAR (87). However, the irregular shape, atypical direction, and number of paravalvular jets seen after TAVR makes assessment using these traditional methods questionable. In addition, 1 of the semiquantitative parameters mentioned in the ASE guidelines (i.e., circumferential extent of the jet) had little validation. Subsequent to this guideline, the updated VARC-2 (Valve Academic Research Consortium) consensus document (88), as well as methods used for the PARTNER trial (89), used different cutoffs for this parameter: no PAR (no regurgitant color flow), a trace (pinpoint jet in AV short axis view), mild (jet arc length is <10% of the AV annulus short axis view circumference), moderate (jet arc length is 10% to 30% of the AV annulus short axis view circumference), and severe (jet arc length is >30% of the AV annulus short axis view circumference) (Figure 18, Online Videos 18, 19 and 20). It is important to note that frequently the jets are multiple and discontinuous. The circumferential extent should be measured as the sum of the separate jets, not the paravalvular arc which includes the nonregurgitant space between jets.

Recent studies using cardiac magnetic resonance (CMR) confirm the limitations of echocardiographic methods. Cawley et al. (90) reported higher interob-server variability of aortic regurgitation quantification by TTE (r = 0.89) compared with CMR (r = 0.99). Abdel-Wahab et al. (91) also compared echocardiographic assessment of PAR with CMR in a subset of patients randomized to receive balloon-expandable and self-expanding valves in the CHOICE (Trans-catheter Heart Valves in High Risk Patients With Severe Aortic Stenosis: Medtronic CoreValve vs Edwards SAPIEN XT) trial. The study found that

echocardiography underestimated PAR severity after TAVR only for the CoreValve device. Most recently, Ribeiro et al. (92) systematically looked at the semi-quantitative, multiparametric approach advocated by the ASE as well as the VARC-2 suggestion of circumferential extent of the PAR jets. The authors found that the multiparametric approach underestimated aortic regurgitation severity using CMR by 1 grade in 59.5% and by 2 grades in 2.4%. Circumferential extent of prosthetic PAR overestimated severity in 38%, exhibiting a poor correlation with CMR regurgitant volume and fraction ($r^2 = 0.32$, $p = 0.084$; $r^2 = 0.36$, $p = 0.054$, respectively).

Although quantitation of PAR by using echocardiography is advocated by all guidelines, the current method is limited by the number of technically difficult measurements, which restricts the applicability of these techniques for intraprocedural use. Quantitation of prosthetic regurgitant volume, effective regurgitant orifice area, and regurgitant fraction should be performed by using ASE methods (87,93). The regurgitant volume should be calculated as the difference between the stroke volume across any nonregurgitant orifice (right ventricular outflow tract or mitral valve) and the stroke volume across the LVOT. Interobserver variability of this calculation is reasonable, although higher than for CMR (90).

3D echocardiography may overcome the limitations of current 2-dimensional (2D) techniques. A recent study compared the 5 VARC-2 2D TTE parameters for assessing TAVR PAR versus 3D TTE-quantified regurgitant volume and fraction, as well as CMR TAVR (94). The narrowest confidence intervals for regurgitant volume and regurgitant fraction were between CMR and 3D TEE; there was no significant difference between these 2 modalities in the moderate and severe grades. Figure 19 (Online Video 21) presents an example of intraprocedural quantification of PAR by using 3D color Doppler.

Central Aortic Regurgitation—Significant central aortic regurgitation following TAVR may require placement of a second THV or valve-in-valve procedure (Figure 20). In a recent study of acute valve-in-valve placement (38), severe central THV regurgitation was due to leaflet malfunction in 54% of cases, malpositioning in 41% of cases, and unknown causes in 5% of cases. Transcatheter leaflet malfunction may occur in a number of situations. Calcium may protrude through the stented valve, impinging leaflet motion. A low-lying THV may leave native leaflet overhanging the THV stent, which can entrap the THV leaflets (Figure 11). Post-dilation may cause eversion of the THV leaflet (although this does not occur with newer iterations of the balloon-expandable valve). Finally, a tilted/canted valve may distort the THV frame and result in severe central aortic regurgitation (Figures 20A and 20B). This complication can be treated successfully with a valve-in-valve procedure (Figure 20C). Transcatheter leaflets may become pinned open by the stiff wire (Figure 21, Online Video 22); this complication frequently resolves with removal of the wire. In the setting of leaflet eversion and before a valve-in-valve procedure, placement of a pigtail catheter in each of the sinuses of the TAVR valve may help in ameliorating the central insufficiency by causing the everted leaflet to close normally. Again, with later iterations of the balloon-expandable valve, the leaflet design prevents this eversion from occurring. Although rarely performed (2.4% of cases in the PARTNER 1 trial), the majority (88.5%) of repeat valves were

performed immediately. When valve-in-valve is performed in the setting of PAR, the etiology was most commonly malpositioning.

Perforation

Perforation of the ventricle can occur from any of the wires or catheters that enter the cavity. Right ventricular perforation from the pacing wire may go undetected until removal of the wire. In Figure 22 (Online Videos 23 and 24), rapid but focal accumulation of pericardial blood was seen on intra-procedural imaging only after removal of the pacing wire, emphasizing the need for continuous imaging throughout the procedure. Perforation of the left ventricle is typically seen immediately, with accumulation of relatively echodense pericardial blood, associated with tamponade physiology (compression of the ventricular or atrial chambers) and hemodynamic collapse. Figure 23A shows an initially undetected left ventricular (LV) perforation in the setting of a transaortic TAVR. This patient was stable for weeks before presenting with progressive dyspnea and a large pseudoaneurysm. Figure 23B shows a LV perforation that occurred in the setting of cardiopulmonary resuscitation after a long pacing run before BAV; perforation likely occurred secondary to the BAV catheter being pushed through the left ventricle during chest compressions. Both TAVR migration and compression have been reported after cardiopulmonary resuscitation. Figure 24 shows an example of the initial circular shape of the THV (Figures 24A and 24B) in a patient with acute rupture requiring chest compressions. Subsequent images reveal a flattening THV (Figures 24C [Online Video 25] and 24D [Online Video 26]), and color Doppler suggested turbulent trans-aortic flow.

Perforation of the cardiac tissue at the proximal or distal border of the THV can lead to unusual intra-cardiac communications. These perforations are likely related to significant calcific protrusions near the edge of the stent. The most common intracardiac shunt is a ventricular septal defect which occurs at the proximal edge of the THV; the offending calcium extends into the LVOT from the right coronary cusp or commissure between the right coronary cusp and the noncoronary cusp (Figure 25, Online Videos 27 and 28) (95–98). Because rupture of the septum in this region will likely also result in malapposition of the edge of the THV, PAR may accompany this complication. Spectral Doppler flow profiles for this unusual ventricular septal defect may thus have prominent diastolic flow, as well as typical systolic flow (Figure 26). The diastolic flow is a result of PAR; flow from the aorta crosses the ventricular septal defect. The systolic flow is a result of the typical ventricular left-to-right flow. Intraprocedural treatment of this complication is limited given the proximity to the new THV; however, transcatheter paravalvular leak closure may reduce the diastolic flow.

Rare cases of muscular ventricular septal defects have also been reported after transapical implantation of the THV (99,100). This complication is due to direct perforation by the apical cannula and can be avoided with imaging of the cannulation site before apical puncture. Using TEE imaging, the surgeon can determine the optimal position of cannulation, avoiding the right ventricle and interventricular septum as well as avoiding the mitral valve apparatus (see Complications unique to transapical TAVR in subsequent text).

Coronary occlusion

Coronary obstruction is related to the displacement of a calcified native AV leaflet into the coronary ostium. A recent meta-analysis (41) reported a <1% incidence of coronary occlusion (range 0.0% to 4.1%). Most of the reported 24 cases presented with persistent severe hypotension (87.5%), although ST-segment changes and ventricular arrhythmias also occurred. The majority of occlusions occurred immediately after valve implantation (83.3%) due to displacement of the calcified native cusp over the coronary ostium. Rarely patients presented within the first few hours after the procedure (8.3%), or within the first 2 days after the procedure (8.3%). Coronary obstruction occurred more frequently in the left coronary artery (LCA) (83.3%) and was successfully treated with percutaneous coronary intervention in 91.3% of cases. Risk factors appeared to be female sex and no previous bypass surgery. The height of the left main above the annulus was on average 10.3 mm (range 7 to >12 mm), and ∼60% of occlusions occurred with a coronary height >10 mm. A narrow aortic root with shallow sinuses of Valsalva (leaving little room to accommodate the calcified native aortic leaflets after valve deployment) may also be an important factor.

Left Main Occlusion—Characterizing “at-risk” anatomy is of paramount importance in avoiding the complication of left main occlusion. Because the LCA lies in the coronal plane, routine 2D echocardiography imaging cannot typically allow measurement of LCA height above the annulus or left coronary cusp length. One method for predicting left main coronary occlusion is to image the coronary artery during the BAV procedure (as discussed earlier) (Figure 5). If the LCA or right coronary artery ostia become occluded by the bulky calcium of the associated coronary cusp during BAV, pre-emptive measures should be considered which enable rapid treatment of an occluded coronary following TAVR. These measures may include positioning a wire or crimped stent in the LCA. Immediate post-TAVR imaging of coronary occlusion by using 2D echocardiography and color Doppler (Figure 27, Online Video 29) with associated regional wall motion abnormalities may prompt confirmation with coronary angiography.

The etiologies of delayed coronary occlusion are theoretical. Late embolization of calcium or low flow with thrombus formation seem plausible. One author postulated that after TAVR, a periaortic hematoma may have formed and resulted in right coronary artery occlusion (101).

Mitral valve regurgitation (acute)

MV Apparatus Compromise (Perforation and Chordal Rupture)—A recent study of Cohort A of the PARTNER I trial showed that among 30-daysurvivorswho had TAVR, moderate to severe mitral regurgitation had improved in 57.7%, was unchanged in 36.5%, and worsened in 5.8% (102). Although the cause of worsening mitral regurgitation could not be delineated in that study, both ruptured chordae resulting in flail leaflets, and mitral leaflet perforation have been reported. The latter may be predicted by a careful assessment of dystrophic calcification on the anterior mitral leaflet and avoidance of a low implantation. Acute but reversible changes in mitral regurgitation may also occur, mainly under 2 circumstances: primary alteration in mitral morphology from wire entanglement (Figure 1) or ruptured chordae (Figure 28, Online Videos 30 and 31) and secondary changes in annular

morphology due to severe ventricular dysfunction (i.e., diffuse ischemia after long pacing runs) or dilation (i.e., acute severe aortic regurgitation).

Significant LVOT gradients may occur in up to 14% of patients after surgical AV replacement (103–107), with a similar hemodynamic disturbance having been reported after TAVR (108) (Figure 29, Online Videos 32 and 33). The mechanism is thought to be related to a small, hypertrophied ventricle and the development of systolic anterior motion of the mitral leaflet. Associated with this finding is significant mitral regurgitation. Patients at risk for this finding include those with a small, hypertrophied ventricle, the use of catecholamines, narrowing of the LVOT, reduced circulating blood volume, and septal hypertrophy. Because of the association with hypotension and increased mortality (105,106), it is important to recognize this entity and avoid inotropes or afterload reduction.

Complications unique to transapical TAVR

Transapical aortic valve implantation of the balloon-expandable THV is performed through a mini left anterior thoracotomy (47,109,110). Fluoroscopic and TEE guidance are recommended to locate the optimal cannulation site as well as guide the procedure. A recent meta-analysis of transapical TAVR studies revealed the following incidence of major adverse events: 30-day mortality (4.7% to 20.8%), cerebrovascular accident (0.0% to 16.3%), major tachyarrhythmia (0.0% to 48.8%), bradyarrhythmia requiring permanent pacemaker insertion (0.0% to 18.7%), cardiac tamponade (0% to 11%), major bleeding (1% to 17%), myocardial infarction (0% to 6%), aortic dissection/rupture (0% to 5%), moderate to severe paravalvular leak (0.7% to 24.0%), cardiopulmonary bypass support (0% to 15%); conversion to surgery (0.0% to 9.5%), and valve-in-valve implantation (0.6% to 8.0%) (111). Numerous studies suggest that the learning curve in this procedure may play a significant role in outcomes (47,112,113).

There are a number of complications that are unique to the transapical approach. Malpositioning of the apical cannulation site risks perforation of the right ventricle, ventricular septum, or papillary muscle (Figure 30, Online Videos 34 and 35). These complications can be avoided by using intra-procedural imaging. Figure 31 shows an example of the surgeon confirming the intended cannulation site. After a limited thoracotomy, the surgeon indicates the site with an apical poke, which is easily identified in 2 orthogonal views with simultaneous multiplane imaging (Figure 31A, Online Video 36). When appropriately identified, wires pass freely into the left ventricle and across the AV (Figure 31B, Online Video 37).

Acute myocardial infarction may occur by either direct or indirect compromise of distal coronary flow. The location of the apical cannulation site is in part dictated by the location of the left anterior descending aorta or associated coronary artery bypass grafts. Perforation of the vessel is thus unlikely given the ability to directly visualize the vessel. However, indirect obstruction of distal coronary flow after cannula removal and apical closure can occur due to tension from the purse-string sutures (114). This rare complication can be first detected by intraprocedural TEE, which shows marked apical hypokinesis involving more than the immediate cannulation site (Figure 32, Online Video 38). Treatment by implanting a coronary stent may be warranted.

Because of the direct cannulation through the ventricular apex, acute laceration and hemorrhage are possible. Direct visualization of the apex during closure should reduce the likelihood of this complication; nonetheless, persistent bleeding and pericardial tamponade may occur. Development of a pseudoaneurysm may result from incomplete closure of the apical cannulation site but may not be detected until well after the procedure (Figure 33, Online Videos 39 and 40).

Malpositioning of the transcatheter valve

Although operator-independent motion of the balloon-expandable valve is usually predictable and has been well described for the first generation and second generation balloon-expandable valves (67), there is rarely an unexpected extreme motion of the valve. Embolization of the valve into the aorta may itself result in aortic trauma, but if not, intentional repositioning of the valve into the descending aorta beyond the great arteries (Figure 34) may be necessary before attempted deployment of a second valve at the aortic annulus. Translocation of the valve into the ventricle can also occur when the initial position of the valve is too low (Figure 35, Online Videos 41 and 42). This complication typically requires open retrieval of the transcatheter valve.

Conclusions

This imaging compendium from the PARTNER trials is a compilation of intraprocedural complications of balloon-expandable THV implantation imaged by using intraprocedural TEE. Although newer iterations of the balloon-expandable valve, as well as other valve designs, may significantly reduce the rate of some complications such as PAR, recognizing, predicting, or effectively reacting to all complications remains an important aspect of improving the safety of TAVR. As the field progresses and lower risk patients are treated, early recognition of complications will remain an important advantage of intraprocedural imaging.

Supplementary Material

Refer to Web version on PubMed Central for supplementary material.

Acknowledgments

Dr. Hahn has Core Lab contracts with Edwards Lifesciences for which she receives no direct compensation; and is a speaker for Philips Healthcare, St. Jude Medical, and Boston Scientific. Dr. Kodali has received consulting fees from Edwards Lifesciences. Dr. Webb has served as a consultant to Edwards Lifesciences. Dr. Thourani has received research support from Edwards Lifesciences. Dr. Douglas has received research grants to her institution. All other authors have reported that they have no relationships relevant to the contents of this paper to disclose.

References

1. Leon MB, Smith CR, Mack M, et al. Transcatheter aortic-valve implantation for aortic stenosis in patients who cannot undergo surgery. N Engl J Med. 2010; 363:1597–607. [PubMed: 20961243]
2. Smith CR, Leon MB, Mack MJ, et al. Transcatheter versus surgical aortic-valve replacement in high-risk patients. N Engl J Med. 2011; 364:2187–98. [PubMed: 21639811]
3. Bonow RO, Carabello BA, Kanu C, et al. ACC/AHA 2006 guidelines for the management of patients with valvular heart disease: a report of the American College of Cardiology/American

Heart Association Task Force on Practice Guidelines (writing committee to revise the 1998 Guidelines for the Management of Patients With Valvular Heart Disease). J Am Coll Cardiol. 2006; 48:598–675.

4. Baumgartner H, Hung J, Bermejo J, et al. Echocardiographic assessment of valve stenosis: EAE/ASE recommendations for clinical practice. J Am Soc Echocardiogr. 2009; 22:1–23. quiz 101–2. [PubMed: 19130998]
5. Santos N, de Agustin JA, Almeria C, et al. Prosthesis/annulus discongruence assessed by three-dimensional transoesophageal echocardiography: a predictor of significant paravalvular aortic regurgitation after transcatheter aortic valve implantation. Eur Heart J Cardiovasc Imaging. 2012; 13:931–7. [PubMed: 22511810]
6. Hahn R, Khalique O, Williams M, et al. Predicting paravalvular regurgitation following transcatheter valve replacement: utility of a novel method for three-dimensional echocardiographic measurements of the aortic annulus. J Am Soc Echocardiogr. 2013; 26:1044–52.
7. Delgado V, Ng AC, Shanks M, et al. Transcatheter aortic valve implantation: role of multi-modality cardiac imaging. Expert Rev Cardiovasc Ther. 2010; 8:113–23. [PubMed: 20030025]
8. Jabbour A, Ismail TF, Moat N, et al. Multimodality imaging in transcatheter aortic valve implantation and post-procedural aortic regurgitation: comparison among cardiovascular magnetic resonance, cardiac computed tomography, and echocardiography. J Am Coll Cardiol. 2011; 58:2165–73. [PubMed: 22078422]
9. Wood DA, Tops LF, Mayo JR, et al. Role of multislice computed tomography in transcatheter aortic valve replacement. Am J Cardiol. 2009; 103:1295–301. [PubMed: 19406275]
10. Tops LF, Wood DA, Delgado V, et al. Noninvasive evaluation of the aortic root with multislice computed tomography implications for transcatheter aortic valve replacement. J Am Coll Cardiol Img. 2008; 1:321–30.
11. Tzikas A, Schultz CJ, Piazza N, et al. Assessment of the aortic annulus by multislice computed tomography, contrast aortography, and transthoracic echocardiography in patients referred for transcatheter aortic valve implantation. Catheter Cardiovasc Interv. 2011; 77:868–75. [PubMed: 20824762]
12. Schultz CJ, Moelker AD, Tzikas A, et al. Cardiac CT: necessary for precise sizing for transcatheter aortic implantation. EuroIntervention. 2010; 6(Suppl G):G6–13. [PubMed: 20542831]
13. Ng AC, Delgado V, van der Kley F, et al. Comparison of aortic root dimensions and geometries before and after transcatheter aortic valve implantation by 2- and 3-dimensional transesophageal echocardiography and multislice computed tomography. Circ Cardiovasc Imaging. 2010; 3:94–102. [PubMed: 19920027]
14. Leipsic J, Gurvitch R, LaBounty TM, et al. Multidetector Computed Tomography in Transcatheter Aortic Valve Implantation. J Am Coll Cardiol Img. 2011; 4:416–29.
15. Koos R, Altiok E, Mahnken AH, et al. Evaluation of aortic root for definition of prosthesis size by magnetic resonance imaging and cardiac computed tomography: implications for transcatheter aortic valve implantation. Int J Cardiol. 2012; 158:353–8. [PubMed: 21315460]
16. Hamdan A, Guetta V, Konen E, et al. Deformation dynamics and mechanical properties of the aortic annulus by 4-dimensional computed tomography insights into the functional anatomy of the aortic valve complex and implications for transcatheter aortic valve therapy. J Am Coll Cardiol. 2012; 59:119–27. [PubMed: 22222074]
17. Delgado V, Ng AC, van de Veire NR, et al. Transcatheter aortic valve implantation: role of multi-detector row computed tomography to evaluate prosthesis positioning and deployment in relation to valve function. Eur Heart J. 2010; 31:1114–23. [PubMed: 20173197]
18. Altiok E, Koos R, Schroder J, et al. Comparison of two-dimensional and three-dimensional imaging techniques for measurement of aortic annulus diameters before transcatheter aortic valve implantation. Heart. 2011; 97:1578–84. [PubMed: 21700756]
19. Zamorano JL, Badano LP, Bruce C, et al. EAE/ASE recommendations for the use of echocardiography in new transcatheter interventions for valvular heart disease. J Am Soc Echocardiogr. 2011; 24:937–65. [PubMed: 21867869]
20. Bloomfield GS, Gillam LD, Hahn RT, et al. A practical guide to multimodality imaging of transcatheter aortic valve replacement. J Am Coll Cardiol Img. 2012; 5:441–55.

21. Smith LA, Dworakowski R, Bhan A, et al. Realtime three-dimensional transesophageal echocardiography adds value to transcatheter aortic valve implantation. J Am Soc Echocardiogr. 2013; 26:359–69. [PubMed: 23484436]
22. Durand E, Borz B, Godin M, et al. Transfemoral aortic valve replacement with the Edwards SAPIEN and Edwards SAPIEN XT prosthesis using exclusively local anesthesia and fluoroscopic guidance: feasibility and 30-day outcomes. J Am Coll Cardiol Intv. 2012; 5:461–7.
23. Bagur R, Rodés-Cabau J, Doyle D, et al. Usefulness of TEE as the primary imaging technique to guide transcatheter transapical aortic valve implantation. J Am Coll Cardiol Img. 2011; 4:115–24.
24. Holmes DR Jr, Mack MJ, Kaul S, et al. 2012 ACCF/AATS/SCAI/STS expert consensus document on transcatheter aortic valve replacement. J Am Coll Cardiol. 2012; 59:1200–54. [PubMed: 22300974]
25. Hahn RT, Abraham T, Adams MS, et al. Guidelines for performing a comprehensive transesophageal echocardiographic examination: recommendations from the american society of echocardiography and the society of cardiovascular anesthesiologists. J Am Soc Echocardiogr. 2013; 26:921–64. [PubMed: 23998692]
26. Greif M, Lange P, Nabauer M, et al. Transcutaneous aortic valve replacement with the Edwards SAPIEN XT and Medtronic CoreValve prosthesis under fluoroscopic guidance and local anaesthesia only. Heart. 2014; 100:691–5. [PubMed: 24459291]
27. Motloch LJ, Rottlaender D, Reda S, et al. Local versus general anesthesia for transfemoral aortic valve implantation. Clin Res Cardiol. 2012; 101:45–53. [PubMed: 21931964]
28. Yamamoto M, Meguro K, Mouillet G, et al. Effect of local anesthetic management with conscious sedation in patients undergoing transcatheter aortic valve implantation. Am J Cardiol. 2013; 111:94–9. [PubMed: 23068861]
29. Babaliaros V, Cribier A. The expansion of transcatheter technology to treat aortic insufficiency: everything old becomes new again. J Am Coll Cardiol Intv. 2014; 7:1175–6.
30. Kodali SK, Williams MR, Smith CR, et al. Two-year outcomes after transcatheter or surgical aortic-valve replacement. N Engl J Med. 2012; 366:1686–95. [PubMed: 22443479]
31. Van Mieghem NM, Nuis RJ, Piazza N, et al. Vascular complications with transcatheter aortic valve implantation using the 18 Fr Medtronic CoreValve System: the Rotterdam experience. EuroIntervention. 2010; 5:673–9. [PubMed: 20142217]
32. Himbert D, Brochet E, Ducrocq G, Vahanian A. Contrast echocardiography guidance for alcohol septal ablation of hypertrophic obstructive cardiomyopathy. Eur Heart J. 2010; 31:1148. [PubMed: 20019022]
33. Kahlert P, Al-Rashid F, Weber M, et al. Vascular access site complications after percutaneous transfemoral aortic valve implantation. Herz. 2009; 34:398–408. [PubMed: 19711036]
34. Genereux P, Reiss GR, Kodali SK, Williams MR, Hahn RT. Periaortic hematoma after transcatheter aortic valve replacement: description of a new complication. Catheter Cardiovasc Interv. 2012; 79:766–76. [PubMed: 21805578]
35. Masson JB, Kovac J, Schuler G, et al. Transcatheter aortic valve implantation: review of the nature, management, and avoidance of procedural complications. J Am Coll Cardiol Intv. 2009; 2:811–20.
36. Sarkar K, Sardella G, Romeo F, et al. Transcatheter aortic valve implantation for severe regurgitation in native and degenerated bio-prosthetic aortic valves. Catheter Cardiovasc Interv. 2013; 81:864–70. [PubMed: 22997004]
37. Al Ali AM, Altwegg L, Horlick EM, et al. Prevention and management of transcatheter balloon-expandable aortic valve malposition. Catheter Cardiovasc Interv. 2008; 72:573–8. [PubMed: 18819120]
38. Makkar RR, Jilaihawi H, Chakravarty T, et al. Determinants and outcomes of acute transcatheter valve-in-valve therapy or embolization: a study of multiple valve implants in the U.S. PARTNER Trial (Placement of AoRTic TraNscathetER Valve Trial Edwards SAPIEN Transcatheter Heart Valve). J Am Coll Cardiol. 2013; 62:418–30. [PubMed: 23684680]
39. Vavouranakis M, Vrachatis DA, Toutouzas KP, Chrysohoou C, Stefanadis C. “Bail out” procedures for malpositioning of aortic valve prosthesis (CoreValve). Int J Cardiol. 2010; 145:154–5. [PubMed: 19716194]

40. Webb JG, Altwegg L, Boone RH, et al. Transcatheter aortic valve implantation: impact on clinical and valve-related outcomes. Circulation. 2009; 119:3009–16. [PubMed: 19487594]
41. Ribeiro HB, Nombela-Franco L, Urena M, et al. Coronary obstruction following transcatheter aortic valve implantation: a systematic review. J Am Coll Cardiol Intv. 2013; 6:452–61.
42. Zahn R, Schiele R, Kilkowski C, Zeymer U. Severe aortic regurgitation after percutaneous transcatheter aortic valve implantation: on the importance to clarify the underlying pathophysiology. Clin Res Cardiol. 2010; 99:193–7. [PubMed: 20041329]
43. Sherif MA, Abdel-Wahab M, Stocker B, et al. Anatomic and procedural predictors of paravalvular aortic regurgitation after implantation of the Medtronic CoreValve bioprosthesis. J Am Coll Cardiol. 2010; 56:1623–9. [PubMed: 21050971]
44. Koos R, Mahnken AH, Dohmen G, et al. Association of aortic valve calcification severity with the degree of aortic regurgitation after transcatheter aortic valve implantation. Int J Cardiol. 2011; 150:142–5. [PubMed: 20350770]
45. Rajani R, Kakad M, Khawaja MZ, et al. Paravalvular regurgitation one year after transcatheter aortic valve implantation. Catheter Cardiovasc Interv. 2010; 75:868–72. [PubMed: 20146320]
46. Colli A, D'Amico R, Kempfert J, Borger MA, Mohr FW, Walther T. Transesophageal echocardiographic scoring for transcatheter aortic valve implantation: impact of aortic cusp calcification on postoperative aortic regurgitation. J Thorac Cardiovasc Surg. 2011; 142:1229–35. [PubMed: 22014345]
47. Unbehaun A, Pasic M, Dreysse S, et al. Transapical aortic valve implantation incidence and predictors of paravalvular leakage and transvalvular regurgitation in a series of 358 patients. J Am Coll Cardiol. 2012; 59:211–21. [PubMed: 22240125]
48. Detaint D, Lepage L, Himbert D, et al. Determinants of significant paravalvular regurgitation after transcatheter aortic valve: implantation impact of device and annulus discongruence. J Am Coll Cardiol Intv. 2009; 2:821–7.
49. Athappan G, Patvardhan E, Tuzcu EM, et al. Incidence, predictors, and outcomes of aortic regurgitation after transcatheter aortic valve replacement: meta-analysis and systematic review of literature. J Am Coll Cardiol. 2013; 61:1585–95. [PubMed: 23500308]
50. Leon MB, Piazza N, Nikolsky E, et al. Standardized endpoint definitions for transcatheter aortic valve implantation clinical trials: a consensus report from the Valve Academic Research Consortium. Eur Heart J. 2011; 32:205–17. [PubMed: 21216739]
51. Nuis RJ, Piazza N, Van Mieghem NM, et al. Inhospital complications after transcatheter aortic valve implantation revisited according to the Valve Academic Research Consortium definitions. Catheter Cardiovasc Interv. 2011; 78:457–67. [PubMed: 21563291]
52. Lang RM, Badano LP, Tsang W, et al. EAE/ASE recommendations for image acquisition and display using three-dimensional echocardiography. J Am Soc Echocardiogr. 2012; 25:3–46. [PubMed: 22183020]
53. Babaliaros VC, Liff D, Chen EP, et al. Can balloon aortic valvuloplasty help determine appropriate transcatheter aortic valve size? J Am Coll Cardiol Intv. 2008; 1:580–6.
54. Patsalis PC, Al-Rashid F, Neumann T, et al. Preparatory balloon aortic valvuloplasty during transcatheter aortic valve implantation for improved valve sizing. J Am Coll Cardiol Intv. 2013; 6:965–71.
55. Kasel AM, Cassese S, Bleiziffer S, et al. Standardized imaging for aortic annular sizing: implications for transcatheter valve selection. J Am Coll Cardiol Img. 2013; 6:249–62.
56. Ben-Dor I, Pichard AD, Satler LF, et al. Complications and outcome of balloon aortic valvuloplasty in high-risk or inoperable patients. J Am Coll Cardiol Intv. 2010; 3:1150–6.
57. Eggebrecht H, Schmermund A, Kahlert P, Erbel R, Voigtlander T, Mehta RH. Emergent cardiac surgery during transcatheter aortic valve implantation (TAVI): a weighted meta-analysis of 9,251 patients from 46 studies. EuroIntervention. 2013; 8:1072–80. [PubMed: 23134947]
58. Latib A, Michev I, Laborde JC, Montorfano M, Colombo A. Post-implantation repositioning of the CoreValve percutaneous aortic valve. J Am Coll Cardiol Intv. 2010; 3:119–21.
59. Schultz CJ, Weustink A, Piazza N, et al. Geometry and degree of apposition of the CoreValve ReValving system with multislice computed tomography after implantation in patients with aortic stenosis. J Am Coll Cardiol. 2009; 54:911–8. [PubMed: 19712801]

60. Schultz CJ, Tzikas A, Moelker A, et al. Correlates on MSCT of paravalvular aortic regurgitation after transcatheter aortic valve implantation using the Medtronic CoreValve prosthesis. Catheter Cardiovasc Interv. 2011; 78:446–55. [PubMed: 21793166]
61. Eggebrecht H, Doss M, Schmermund A, Nowak B, Krissel J, Voigtlander T. Interventional options for severe aortic regurgitation after transcatheter aortic valve implantation: balloons, snares, valve-in-valve. Clin Res Cardiol. 2012; 101:503–7. [PubMed: 22476821]
62. Block PC. Leaks and the “great ship” TAVI. Catheter Cardiovasc Interv. 2010; 75:873–4. [PubMed: 20432392]
63. Lerakis S, Hayek SS, Douglas PS. Paravalvular aortic leak after transcatheter aortic valve replacement: current knowledge. Circulation. 2013; 127:397–407. [PubMed: 23339094]
64. Genereux P, Head SJ, Hahn R, et al. Paravalvular leak after transcatheter aortic valve replacement: the new Achilles' heel? A comprehensive review of the literature. J Am Coll Cardiol. 2013; 61:1125–36. [PubMed: 23375925]
65. Nuis RJ, Van Mieghem NM, Schultz CJ, et al. Timing and potential mechanisms of new conduction abnormalities during the implantation of the Medtronic CoreValve System in patients with aortic stenosis. Eur Heart J. 2011; 32:2067–74. [PubMed: 21622979]
66. Saia F, Lemos PA, Bordoni B, et al. Transcatheter aortic valve implantation with a self-expanding nitinol bioprosthesis: prediction of the need for permanent pacemaker using simple baseline and procedural characteristics. Catheter Cardiovasc Interv. 2012; 79:712–9. [PubMed: 22109957]
67. Dvir D, Lavi I, Eltchaninoff H, et al. Multicenter Evaluation of Edwards SAPIEN Positioning During Transcatheter Aortic Valve Implantation With Correlates for Device Movement During Final Deployment. J Am Coll Cardiol Intv. 2012; 5:563–70.
68. Cao C, Ang SC, Vallely MP, Ng M, Adams M, Wilson M. Migration of the transcatheter valve into the left ventricle. Ann Cardiothorac Surg. 2012; 1:243–4. [PubMed: 23977502]
69. Webb JG, Pasupati S, Humphries K, et al. Percutaneous transarterial aortic valve replacement in selected high-risk patients with aortic stenosis. Circulation. 2007; 116:755–63. [PubMed: 17646579]
70. Clavel MA, Dumont E, Pibarot P, et al. Severe valvular regurgitation and late prosthesis embolization after percutaneous aortic valve implantation. Ann Thorac Surg. 2009; 87:618–21. [PubMed: 19161796]
71. Maroto LC, Rodriguez JE, Cobiella J, Silva J. Delayed dislocation of a transapically implanted aortic bioprosthesis. Eur J Cardiothorac Surg. 2009; 36:935–7. [PubMed: 19643623]
72. Pang PY, Chiam PT, Chua YL, Sin YK. A survivor of late prosthesis migration and rotation following percutaneous transcatheter aortic valve implantation. Eur J Cardiothorac Surg. 2012; 41:1195–6. [PubMed: 22228843]
73. Barbanti M, Yang TH, Rodés-Cabau J, et al. Anatomical and procedural features associated with aortic root rupture during balloon-expandable transcatheter aortic valve replacement. Circulation. 2013; 128:244–53. [PubMed: 23748467]
74. Harris KM, Braverman AC, Eagle KA, et al. Acute aortic intramural hematoma: an analysis from the International Registry of Acute Aortic Dissection. Circulation. 2012; 126(Suppl 1):S91–6. [PubMed: 22965999]
75. Abdel-Wahab M, Zahn R, Horack M, et al. Aortic regurgitation after transcatheter aortic valve implantation: incidence and early outcome. Results from the German Transcatheter Aortic Valve Interventions registry. Heart. 2011; 97:899–906. [PubMed: 21398694]
76. Tamburino C, Capodanno D, Ramondo A, et al. Incidence and predictors of early and late mortality after transcatheter aortic valve implantation in 663 patients with severe aortic stenosis. Circulation. 2011; 123:299–308. [PubMed: 21220731]
77. Moat NE, Ludman P, de Belder MA, et al. Long-term outcomes after transcatheter aortic valve implantation in high-risk patients with severe aortic stenosis: the U.K. TAVI (United Kingdom Transcatheter Aortic Valve Implantation) Registry. J Am Coll Cardiol. 2011; 58:2130–8. [PubMed: 22019110]
78. Gotzmann M, Korten M, Bojara W, et al. Long-term outcome of patients with moderate and severe prosthetic aortic valve regurgitation after transcatheter aortic valve implantation. Am J Cardiol. 2012; 110:1500–6. [PubMed: 22863177]

79. Sinning JM, Hammerstingl C, Vasa-Nicotera M, et al. Aortic regurgitation index defines severity of peri-prosthetic regurgitation and predicts outcome in patients after transcatheter aortic valve implantation. J Am Coll Cardiol. 2012; 59:1134–41. [PubMed: 22440213]
80. Hayashida K, Morice MC, Chevalier B, et al. Sex-related differences in clinical presentation and outcome of transcatheter aortic valve implantation for severe aortic stenosis. J Am Coll Cardiol. 2012; 59:566–71. [PubMed: 22300690]
81. Ewe SH, Ng AC, Schuijf JD, et al. Location and severity of aortic valve calcium and implications for aortic regurgitation after transcatheter aortic valve implantation. Am J Cardiol. 2011; 108:1470–7. [PubMed: 21855831]
82. Nombela-Franco L, Rodés-Cabau J, DeLarochelliere R, et al. Predictive factors, efficacy, and safety of balloon post-dilation after transcatheter aortic valve implantation with a balloon-expandable valve. J Am Coll Cardiol Intv. 2012; 5:499–512.
83. Schultz C, Rossi A, van Mieghem N, et al. Aortic annulus dimensions and leaflet calcification from contrast MSCT predict the need for balloon post-dilatation after TAVI with the Medtronic CoreValve prosthesis. EuroIntervention. 2011; 7:564–72. [PubMed: 21930460]
84. Marwan M, Achenbach S, Ensminger SM, et al. CT predictors of post-procedural aortic regurgitation in patients referred for transcatheter aortic valve implantation: an analysis of 105 patients. Int J Cardiovasc Imaging. 2013; 29:1191–8. [PubMed: 23420354]
85. Gripari P, Ewe SH, Fusini L, et al. Intra-operative 2D and 3D transoesophageal echocardiographic predictors of aortic regurgitation after transcatheter aortic valve implantation. Heart. 2012; 98:1229–36. [PubMed: 22826560]
86. John D, Buellesfeld L, Yuecel S, et al. Correlation of Device landing zone calcification and acute procedural success in patients undergoing transcatheter aortic valve implantations with the self-expanding CoreValve prosthesis. J Am Coll Cardiol Intv. 2010; 3:233–43.
87. Zoghbi WA, Enriquez-Sarano M, Foster E, et al. Recommendations for evaluation of the severity of native valvular regurgitation with two-dimensional and Doppler echocardiography. J Am Soc Echocardiogr. 2003; 16:777–802. [PubMed: 12835667]
88. Kappetein AP, Head SJ, Genereux P, et al. Updated standardized endpoint definitions for transcatheter aortic valve implantation: the Valve Academic Research Consortium-2 consensus document. J Am Coll Cardiol. 2012; 60:1438–54. [PubMed: 23036636]
89. Douglas PS, Waugh RA, Bloomfield G, et al. Implementation of echocardiography core laboratory best practices: a case study of the PARTNER I trial. J Am Soc Echocardiogr. 2013; 26:348–58. e3. [PubMed: 23465887]
90. Cawley PJ, Hamilton-Craig C, Owens DS, et al. Prospective comparison of valve regurgitation quantitation by cardiac magnetic resonance imaging and transthoracic echocardiography. Circ Cardiovasc Imaging. 2013; 6:48–57. [PubMed: 23212272]
91. Abdel-Wahab M, Mehilli J, Frerker C, et al. Comparison of balloon-expandable vs self-expandable valves in patients undergoing transcatheter aortic valve replacement: the CHOICE randomized clinical trial. JAMA. 2014; 311:1503–14. [PubMed: 24682026]
92. Ribeiro HB, Le Ven F, Larose E, et al. Cardiac magnetic resonance versus transthoracic echocardiography for the assessment and quantification of aortic regurgitation in patients undergoing transcatheter aortic valve implantation. Heart. 2014; 100:1924–32. [PubMed: 25124218]
93. Zoghbi WA, Chambers JB, Dumesnil JG, et al. Recommendations for evaluation of prosthetic valves with echocardiography and Doppler ultrasound: a report From the American Society of Echocardiography's Guidelines and Standards Committee and the Task Force on Prosthetic Valves. J Am Soc Echocardiogr. 2009; 22:975–1014. quiz 82–4. [PubMed: 19733789]
94. Altiok E, Frick M, Meyer CG, et al. Comparison of two- and three-dimensional transthoracic echocardiography to cardiac magnetic resonance imaging for assessment of paravalvular regurgitation after transcatheter aortic valve implantation. Am J Cardiol. 2014; 113:1859–66. [PubMed: 24837265]
95. Patel Y, Vassileva C, Mishkel G. Rare complication of ventricular septal defect in three patients following transcatheter aortic valve replacement. Catheter Cardiovasc Interv. 2014; 83:497–501. [PubMed: 24123754]

96. Tzikas A, Schultz C, Piazza N, van Geuns RJ, Serruys PW, de Jaegere PP. Perforation of the membranous interventricular septum after transcatheter aortic valve implantation. Circ Cardiovasc Interv. 2009; 2:582–3. [PubMed: 20031778]

97. Gerckens U, Latsios G, Pizzulli L. Percutaneous treatment of a post-TAVI ventricular septal defect: a successful combined procedure for an unusual complication. Catheter Cardiovasc Interv. 2013; 81:E274–7. [PubMed: 22581693]

98. Aminian A, Lalmand J, Dolatabadi D. Late contained aortic root rupture and ventricular septal defect after transcatheter aortic valve implantation. Catheter Cardiovasc Interv. 2013; 81:E72–5. [PubMed: 22431403]

99. Al-Attar N, Ghodbane W, Himbert D, et al. Unexpected complications of transapical aortic valve implantation. Ann Thorac Surg. 2009; 88:90–4. [PubMed: 19559200]

100. Massabuau P, Dumonteil N, Berthoumieu P, et al. Left-to-right interventricular shunt as a late complication of transapical aortic valve implantation. J Am Coll Cardiol Intv. 2011; 4:710–2.

101. Kukucka M, Pasic M, Dreysse S, Hetzer R. Delayed subtotal coronary obstruction after transapical aortic valve implantation. Interact Cardiovasc Thorac Surg. 2011; 12:57–60. [PubMed: 21098421]

102. Barbanti M, Webb JG, Hahn RT, et al. Impact of preoperative moderate/severe mitral regurgitation on 2-year outcome after transcatheter and surgical aortic valve replacement: insight from the PARTNER (Placement of AoRTic TraNscathetER Valve) Trial Cohort A. Circulation. 2013; 128:2776–84. [PubMed: 24152861]

103. Bartunek J, Sys SU, Rodrigues AC, van Schuerbeeck E, Mortier L, de Bruyne B. Abnormal systolic intraventricular flow velocities after valve replacement for aortic stenosis. Mechanisms, predictive factors, and prognostic significance. Circulation. 1996; 93:712–9. [PubMed: 8641000]

104. Laurent M, Leborgne O, Clement C, et al. Systolic intra-cavitary gradients following aortic valve replacement: an echo-Doppler study. Eur Heart J. 1991; 12:1098–106. [PubMed: 1782936]

105. Aurigemma G, Battista S, Orsinelli D, Sweeney A, Pape L, Cuenoud H. Abnormal left ventricular intracavitary flow acceleration in patients undergoing aortic valve replacement for aortic stenosis. A marker for high postoperative morbidity and mortality. Circulation. 1992; 86:926–36. [PubMed: 1516206]

106. Wiseth R, Skjaerpe T, Hatle L. Rapid systolic intraventricular velocities after valve replacement for aortic stenosis. Am J Cardiol. 1993; 71:944–8. [PubMed: 8465786]

107. Schwinger ME, O'Brien F, Freedberg RS, Kronzon I. Dynamic left ventricular outflow obstruction after aortic valve replacement: a Doppler echocardiographic study. J Am Soc Echocardiogr. 1990; 3:205–8. [PubMed: 2372403]

108. Takeda Y, Nakatani S, Kuratani T, et al. Systolic anterior motion of the mitral valve and severe mitral regurgitation immediately after transcatheter aortic valve replacement. J Echocardiogr. 2012; 10:143–5.

109. Walther T, Dewey T, Borger MA, Kempfert J, Linke A, Becht R, et al. Transapical aortic valve implantation: step by step. Ann Thorac Surg. 2009; 87:276–83. [PubMed: 19101311]

110. Zierer A, Wimmer-Greinecker G, Martens S, Moritz A, Doss M. The transapical approach for aortic valve implantation. J Thorac Cardiovasc Surg. 2008; 136:948–53. [PubMed: 18954635]

111. Rahnavardi M, Santibanez J, Sian K, Yan TD. A systematic review of transapical aortic valve implantation. Ann Cardiothorac Surg. 2012; 1:116–28. [PubMed: 23977482]

112. Ye J, Cheung A, Lichtenstein SV, et al. Transapical transcatheter aortic valve implantation: follow-up to 3 years. J Thorac Cardiovasc Surg. 2010; 139:1107–13, 13 e1. [PubMed: 20412948]

113. D'Onofrio A, Rubino P, Fusari M, et al. Clinical and hemodynamic outcomes of “all-comers” undergoing transapical aortic valve implantation: results from the Italian Registry of Trans-Apical Aortic Valve Implantation (I-TA). J Thorac Cardiovasc Surg. 2011; 142:768–75. [PubMed: 21840020]

114. Dvir D, Assali A, Porat E, Kornowski R. Distal left anterior descending coronary artery obstruction: a rare complication of transapical aortic valve implantation. J Invasive Cardiol. 2011; 23:E281–3. [PubMed: 22147409]

Abbreviations and Acronyms

AV	aortic valve
CMR	cardiac magnetic resonance
LCA	left coronary artery
LV	left ventricular
PAR	paravalvular aortic regurgitation
TAVR	transcatheter aortic valve replacement
TEE	transesophageal echocardiography
THV	transcatheter heart valve

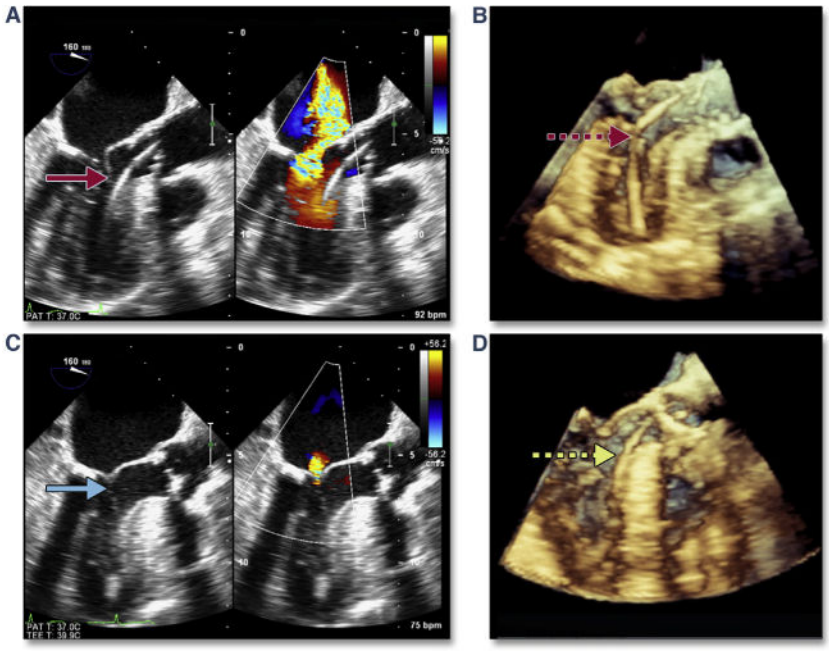

Figure 1. Acute Severe Mitral Regurgitation

During stiff wire positioning, malcoaptation of the mitral valve leaflet (**A, red arrow**) (Online Video 1), resulting in severe mitral regurgitation, may be the first clue to entanglement of the wire in the mitral apparatus (**B, dashed red arrow**). With repositioning of the wire, coaptation of the mitral valve is now normal (**C, blue arrow**) with mild mitral regurgitation. The correct position of the wire is confirmed by using 3-dimensional imaging (**D, dashed yellow arrow**).

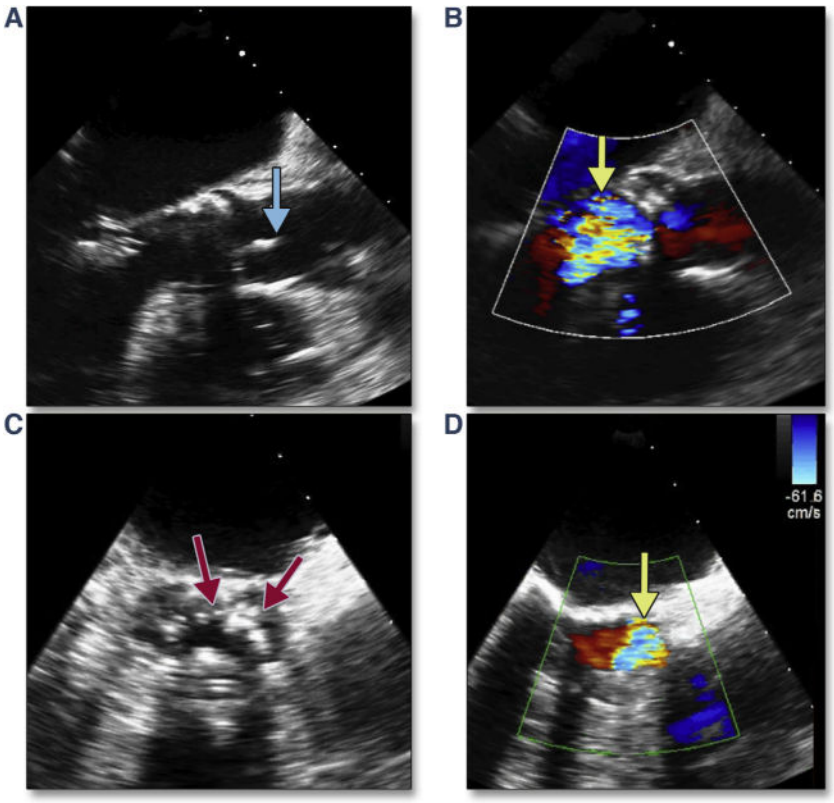

Figure 2. Complications of BAV

Long axis views immediately after balloon aortic valvuloplasty (BAV) show an avulsed leaflet seen in systole **(A, blue arrow)** (Online Video 2), resulting in severe aortic regurgitation in diastole **(B, yellow arrow)**. Short axis views immediately after BAV show immobile aortic cusps in an "open" position **(C, red arrows)** (Online Video 3), resulting in severe aortic regurgitation in diastole **(D, yellow arrow)**.

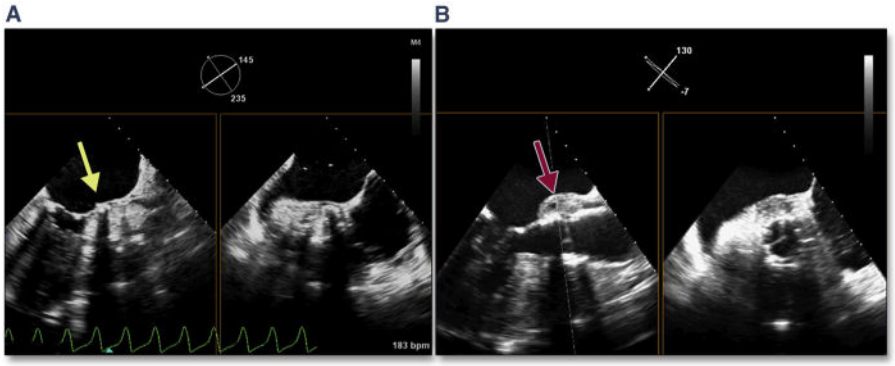

Figure 3. Aortic Trauma Predicted by BAV

Bulky calcified cusps cause deformation of the root during BAV **(A, yellow arrow)** (Online Video 4). This patient suffered a periaortic hematoma within minutes of transcatheter valve deployment **(B, red arrow)** (Online Video 5). Abbreviation as in Figure 2.

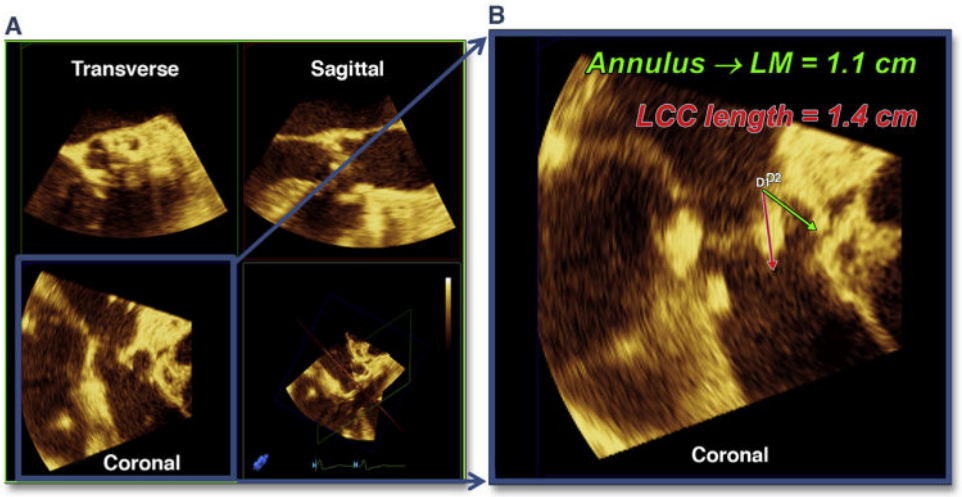

Figure 4. Intraprocedural Measurement of the LM Coronary Height (Above the Annulus) and Length of the LCC by Using 3D Echocardiography

(A) Shows multiplanar reconstruction of the 3-dimensional (3D) volume into the transverse, sagittal, and coronal planes. Typically, the coronal plane must be used to simultaneously image the annulus-to-left main (LM) height **(B)**. LCC = left coronary cusp.

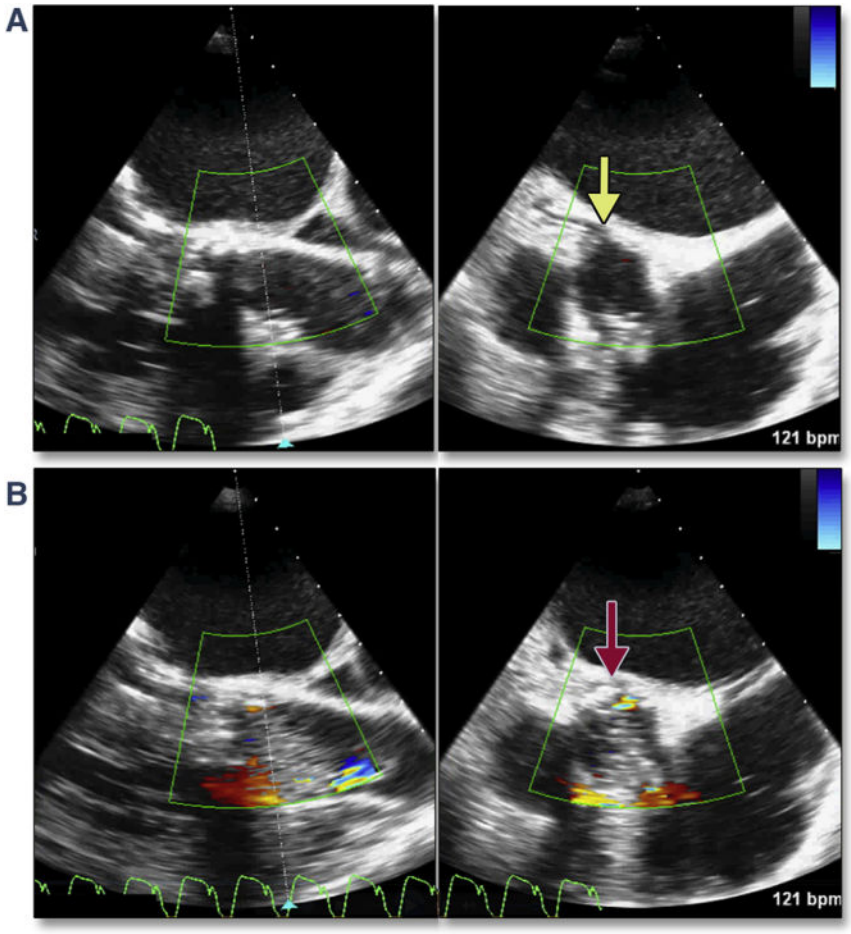

Figure 5. LM Coronary Artery Occlusion Predicted by BAV

Simultaneous multiplane imaging shows the patent LM coronary artery **(A, yellow arrow)** (Online Video 6). With balloon inflation during BAV **(B)** the bulky calcium of the LCC occludes the ostium **(red arrow)**. This patient required a LM stent immediately after transcatheter aortic valve replacement (TAVR). Abbreviations as in Figures 2 and 4.

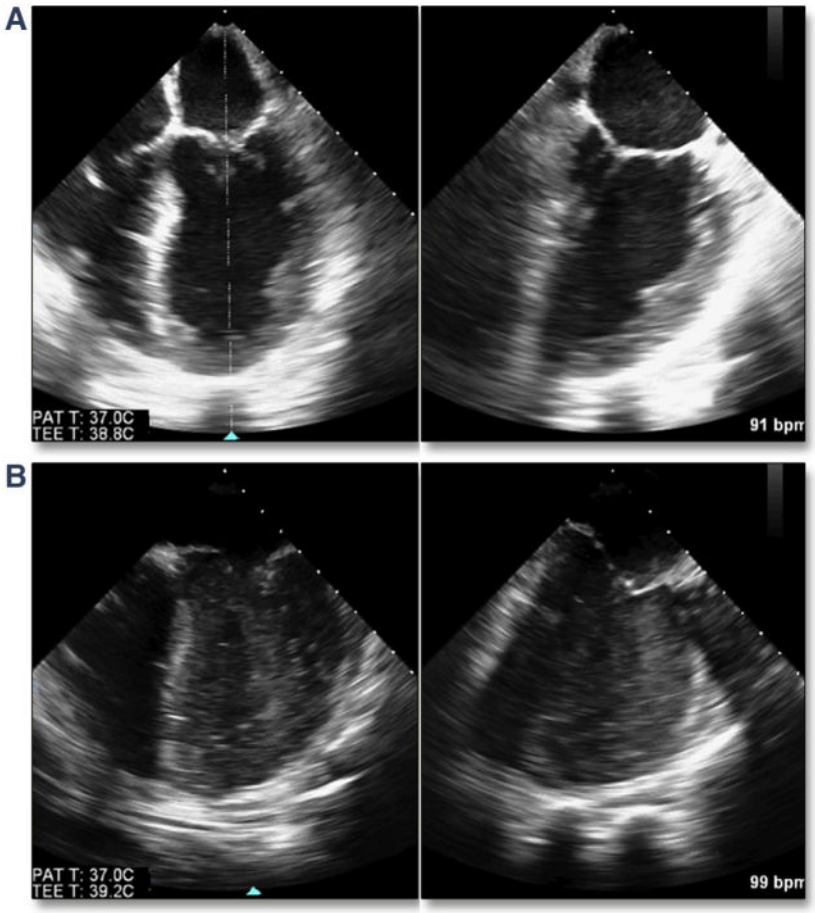

Figure 6. Acute Hemodynamic Collapse

Baseline ventricular function was normal in simultaneous multiplane imaging **(A);** however, after a prolonged pacing run during valve deployment, there was severe significant ventricular dysfunction **(B)** with resulting dense spontaneous contrast (slow flow) secondary to low cardiac output.

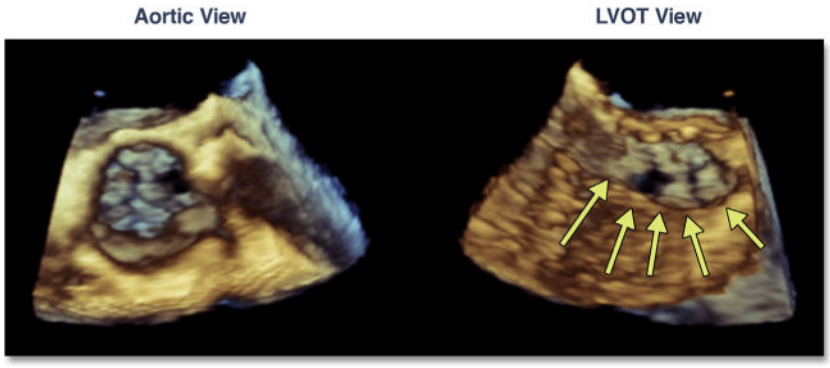

Figure 7. Septal Hypertrophy and Dynamic Narrowing of the LVOT

In this dual-plane 3-dimensional image of the aortic valve, dynamic narrowing of the left ventricular outflow tract (LVOT) can be seen **(yellow arrows)** (Online Video 7).

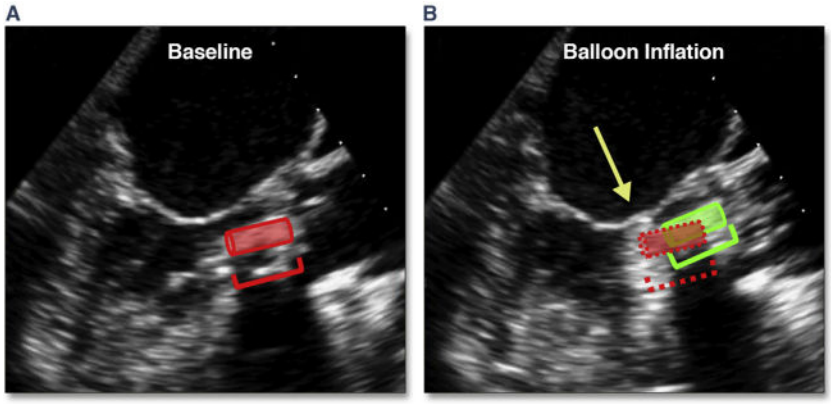

Figure 8. Operator-Independent Motion of the THV Due to Dynamic Narrowing of the LVOT

In **(A)** the position of the transcatheter heart valve (THV) can be seen **(red insert and cartoon)**. With balloon inflation during deployment **(B)**, there is prominent superior motion of the THV **(green insert and cartoon)**, which results in positioning of the THV above the annulus **(yellow arrow)** (Online Video 8). Abbreviation as in Figure 7.

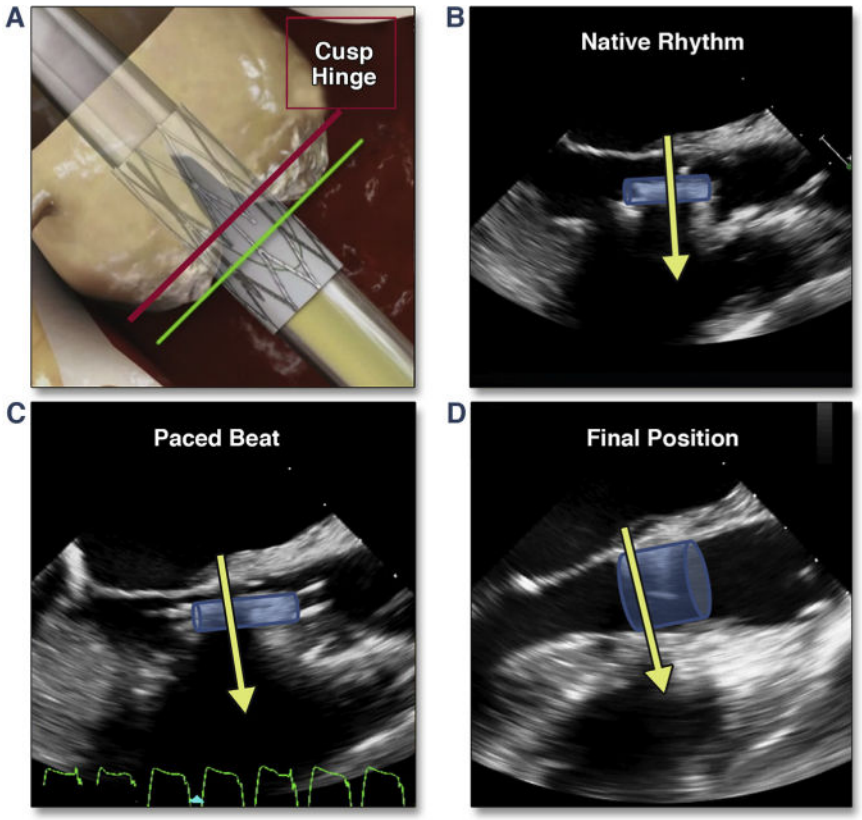

Figure 9. Positioning of the THV

(A) (modified from Dvir et al. [67]) shows the desired fluoroscopic position of the valve just before balloon inflation (during rapid pacing). **(B)** shows the transesophageal echocardiographic position during native rhythm and in diastole, which results in a superior positioning during pacing **(C)**. Shortening of the valve results in positioning of the proximal edge of the THV 1 to 2 mm below the native annulus **(D)** (Online Video 9). Abbreviation as in Figure 8.

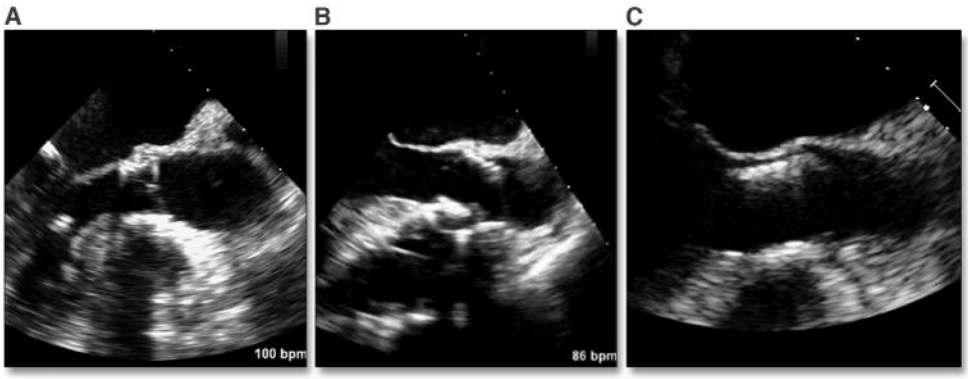

Figure 10. Malpositioning of the Valve

(A) shows a well-positioning valve with typically 20% of the valve below the native annulus. **(B)** shows a valve position into the aorta (see also Figure 20). **(C)** shows a valve positioned within the LVOT. Abbreviation as in Figure 7.

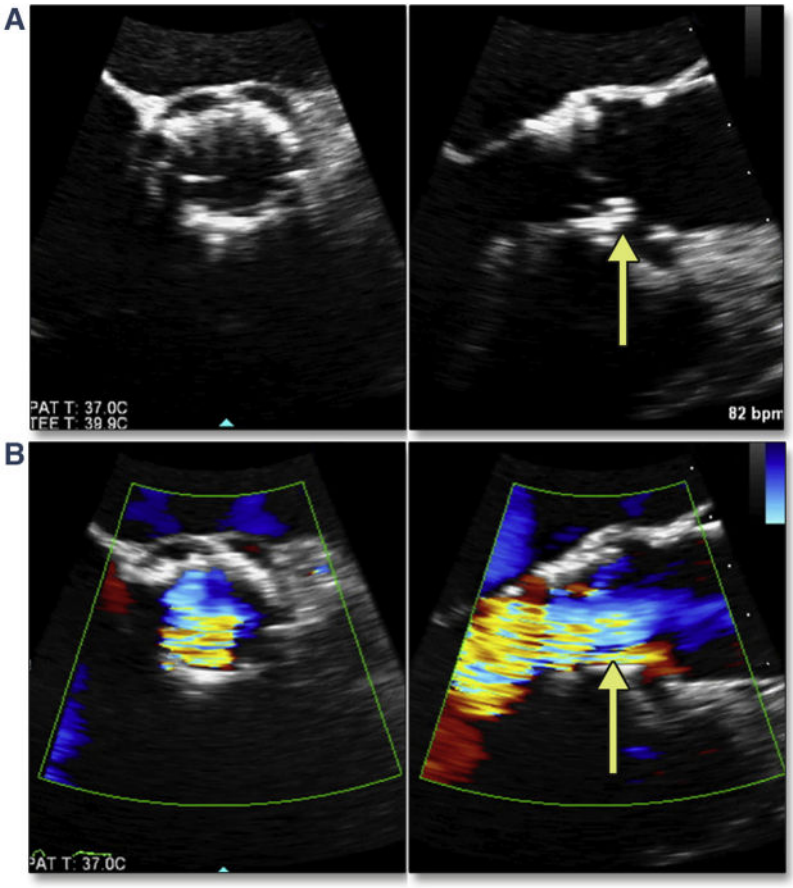

Figure 11. Malpositioning of the THV

Positioning of the THV too ventricular (low), with failure to cover the native cusps, risks native leaflet overhang. In this simultaneous multiplane image, the THV leaflet has become entrapped by the bulky calcium of the overhanging native cusp **(A, yellow arrow)** (Online Video 10), resulting in significant aortic regurgitaton **(B, yellow arrow)** (Online Video 11). Abbreviation as in Figure 8.

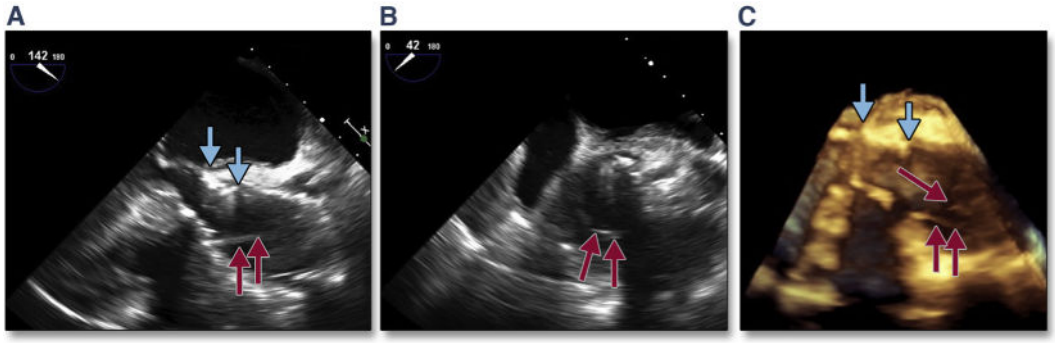

Figure 12. Acute Proximal Aortic Dissection

The transcatheter valve **(A and C, blue arrows)** is well positioned; however, a dissection flap is seen **(red arrows)** from long axis **(A)** and short axis **(B)** views. The complex nature of the dissection is only appreciated by 3-dimensional imaging **(C, multiple red arrows)** (Online Video 12). This complication led to acute tamponade requiring open heart surgery.

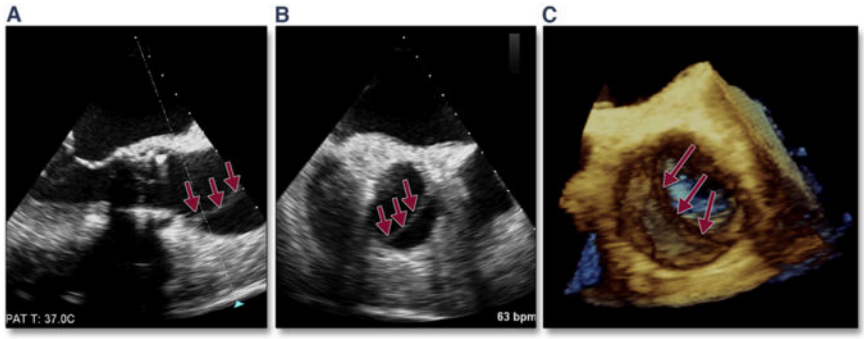

Figure 13. Delayed Proximal Aortic Dissection

A proximal aortic dissection was diagnosed late (>6 months) after TAVR by using 2-dimensional **(A and B)** and 3-dimensional **(C)** (Online Video 13) imaging. The dissection flap **(red arrows)** extends to the sinotubular junction but not into the sinuses, and the patient was treated conservatively. Abbreviation as in Figure 5.

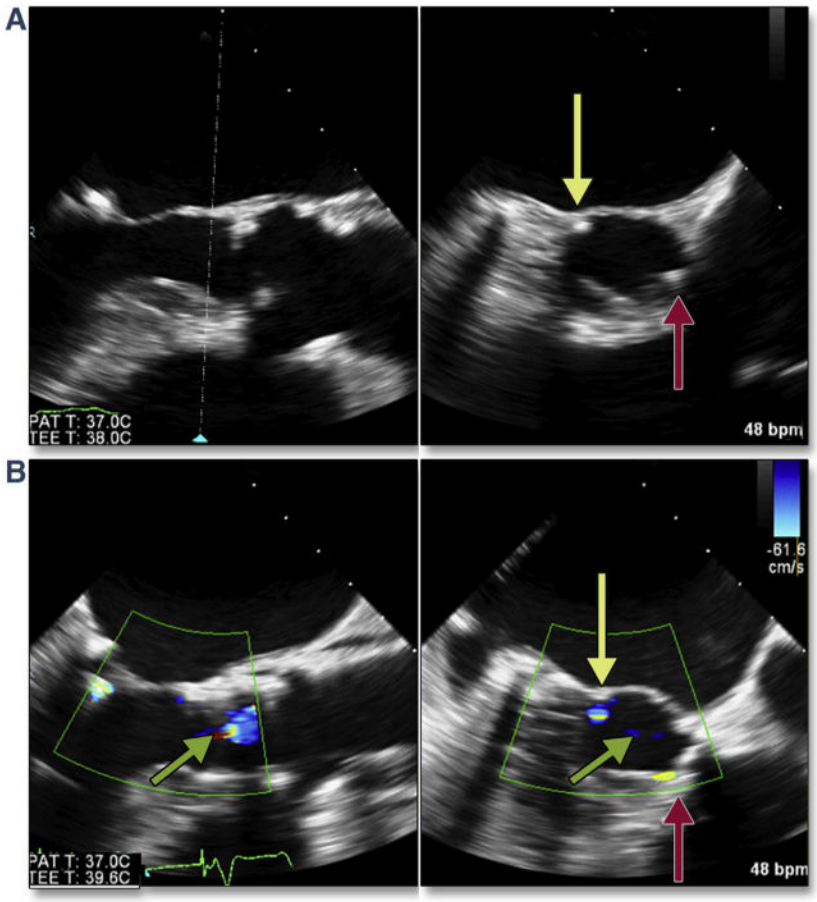

Figure 14. LVOT Calcium and Risk of PAR

Using simultaneous multiplane imaging from the long-axis view **(A)** (Online Video 14), the level of orthogonal imaging plane (indicated by the **dotted white line**) is in the LVOT. LVOT calcium is seen in the short-axis view **(yellow arrow)** with a wire also across the valve **(red arrow)**. After TAVR **(B)** (Online Video 15), a small jet of PAR **(yellow arrow)** was noted adjacent to the LVOT calcium. The mild central regurgitation **(green arrow)** resolved once the wire was removed. PAR = paravalvular aortic regurgitation; other abbreviations as in Figures 5 and 7.

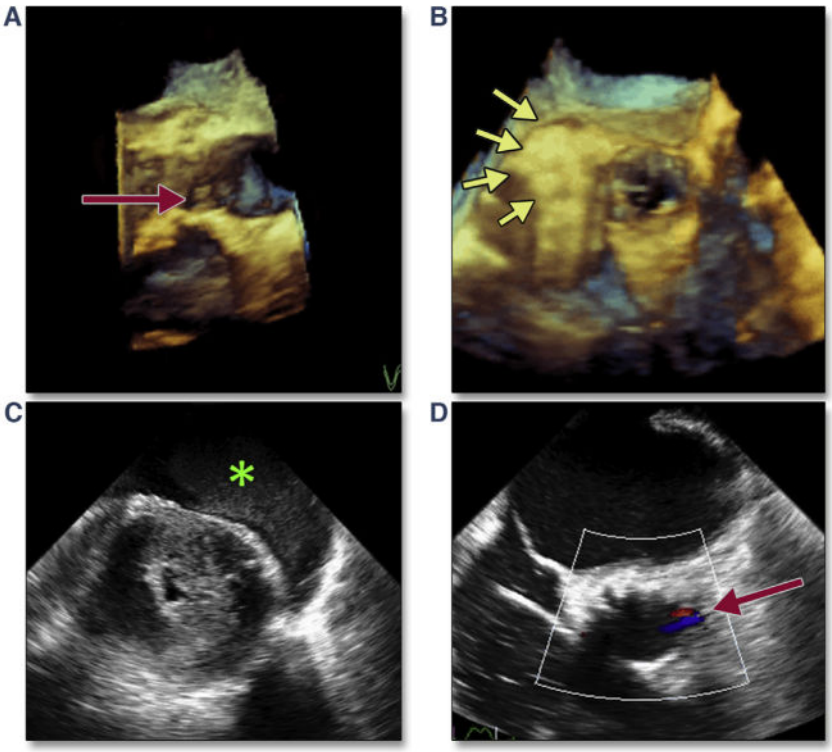

Figure 15. LVOT Calcium and Risk of Annular Rupture

Immediately after TAVR, the severe dystrophic calcification extending from the left coronary cusp into the LVOT caused annular disruption, which is easily imaged on 3-dimensional (3D) reconstruction **(A, red arrow)**. Immediately after deployment, a periaortic hematoma **(B, yellow arrows)** (Online Video 16) and rapidly accumulating pericardial effusion **(C, green asterisk)** are seen. Color Doppler showed abnormal flow originating from the annulus but directed into the center of the LVOT **(D, red arrow)** (Online Video 17). Abbreviations as in Figures 5 and 7.

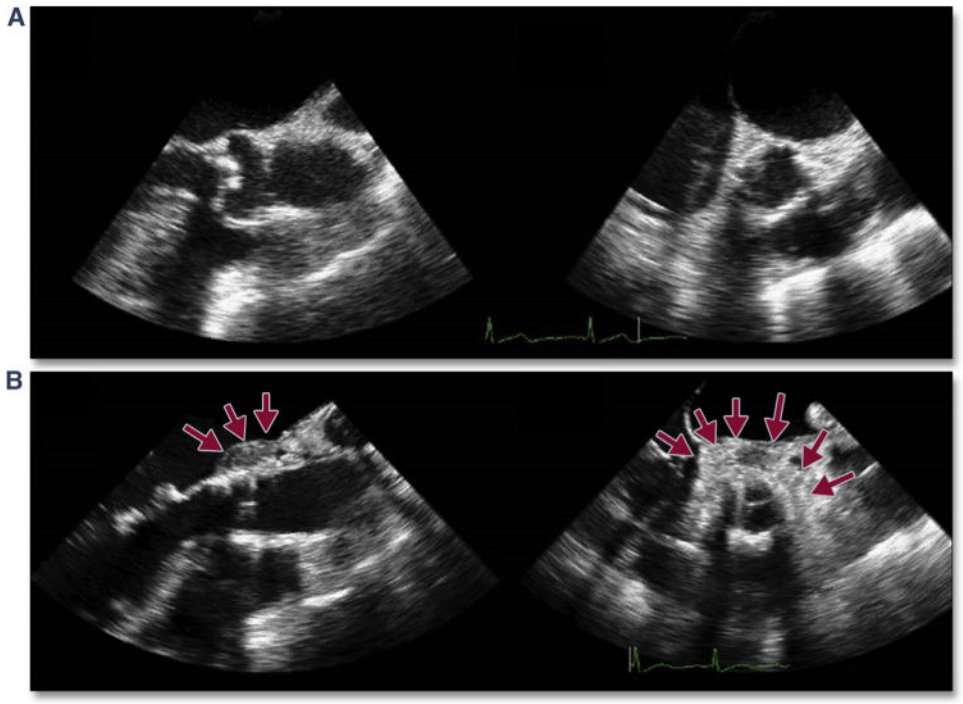

Figure 16. Periaortic Hematoma

A self-limited microperforation of all 3 layers of the aorta may result in a hematoma forming around the outside of the aortic root. **(A)** shows a simultaneous multiplane image of the native aortic root, and **B (red arrows)** shows the self-contained periaortic hematoma which formed after transcatheter aortic valve replacement, contained by the aortic adventitia. Failure to recognize and appropriately respond to this complication may result in continued bleeding into the adventitial space and aortic rupture.

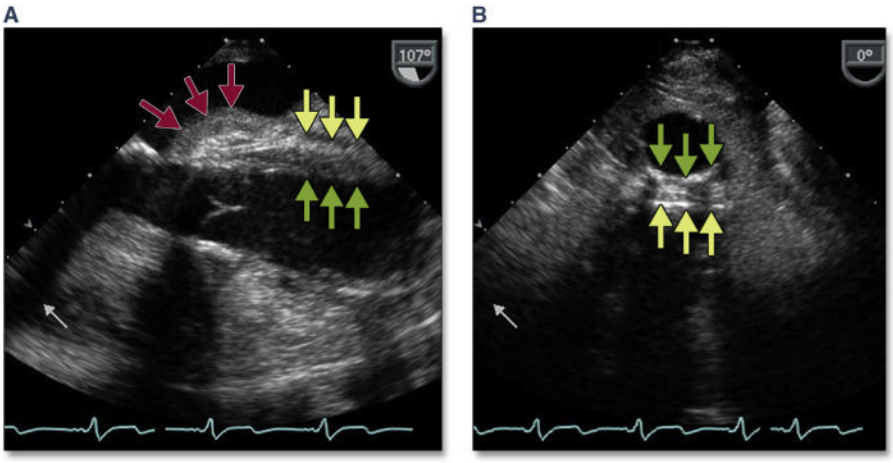

Figure 17. Intramural Hematoma

Bleeding into the wall of the aorta is seen as thickening of the wall between the adventitia **(yellow arrows)** and endothelium **(green arrows)**. In the long axis view **(A)**, this may be associated with periaortic hematoma **(red arrows)**. **(B)** shows extension into the descending aorta with a circumferential thickening of the wall.

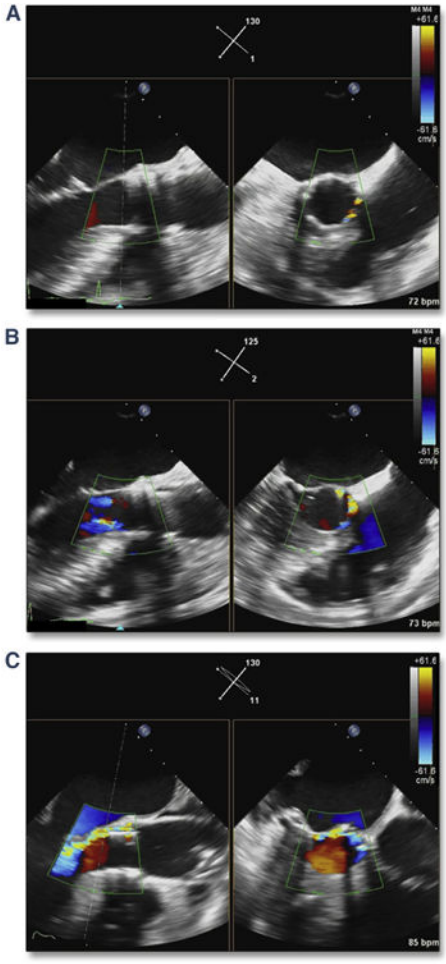

Figure 18. Grading of PAR by Circumferential Extent of the Jet From Short Axis Views

Assessment of the circumferential extent of PAR should be performed just below the THV stent (within the LVOT). No PAR (no regurgitant color flow) is defined as a trace (pinpoint jet in aortic valve short axis view). **(A)** (Online Video 18) shows mild PAR (jet arc lengths are discontinuous, but total <10% of the aortic valve [AV] annulus short axis view circumference). **(B)** (Online Video 19) shows moderate PAR (jet arc lengths are discontinuous, but total 10% to 30% of the AV annulus short axis view circumference). **(C)** (Online Video 20) shows severe PAR (jet arc lengths are discontinuous, but total >30% of the AV annulus short axis view circumference). Abbreviations as in Figures 7, 8, and 14.

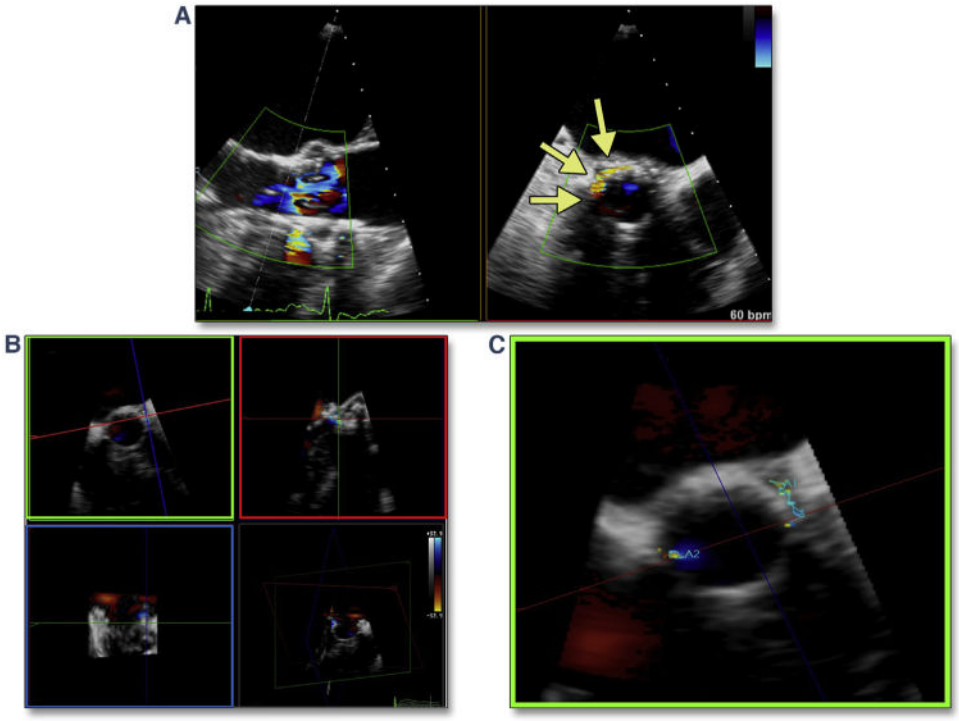

Figure 19. 3D Color Doppler Quantitation of PAR

(A) Simultaneous multiplane 2-dimensional imaging of PAR **(yellow arrows)**, which by circumferential extent suggests moderate to severe PAR (Online Video 21). **(B)** Multiplanar reconstruction of the 3-dimensional (3D) color Doppler jet. **(C)** The 3D planimetry of the narrow, irregularly shaped jet, which measures 6 mm^2 at the vena contracta consistent with mild PAR. Abbreviation as in Figure 14.

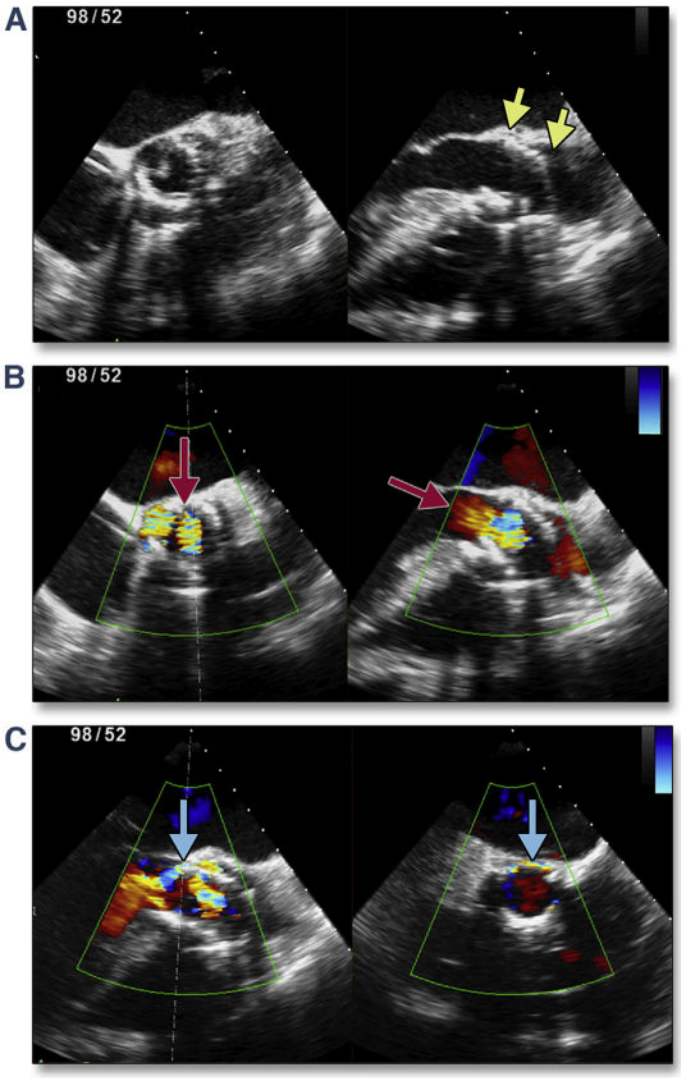

Figure 20. Malposition of the THV and Central Aortic Regurgitation

Severe tilting/canting of the transcatheter valve **(yellow arrows)** occurred in the setting of operator-independent motion of the valve during balloon inflation **(A)**. This malpositioning prevents normal closure of the valve, resulting in severe central aortic regurgitation **(B, red arrows)**. After placement of a second transcatheter valve (valve-in-valve salvage), there was no central regurgitation but moderate paravalvular regurgitation was seen **(C, blue arrows)**. Abbreviation as in Figure 8.

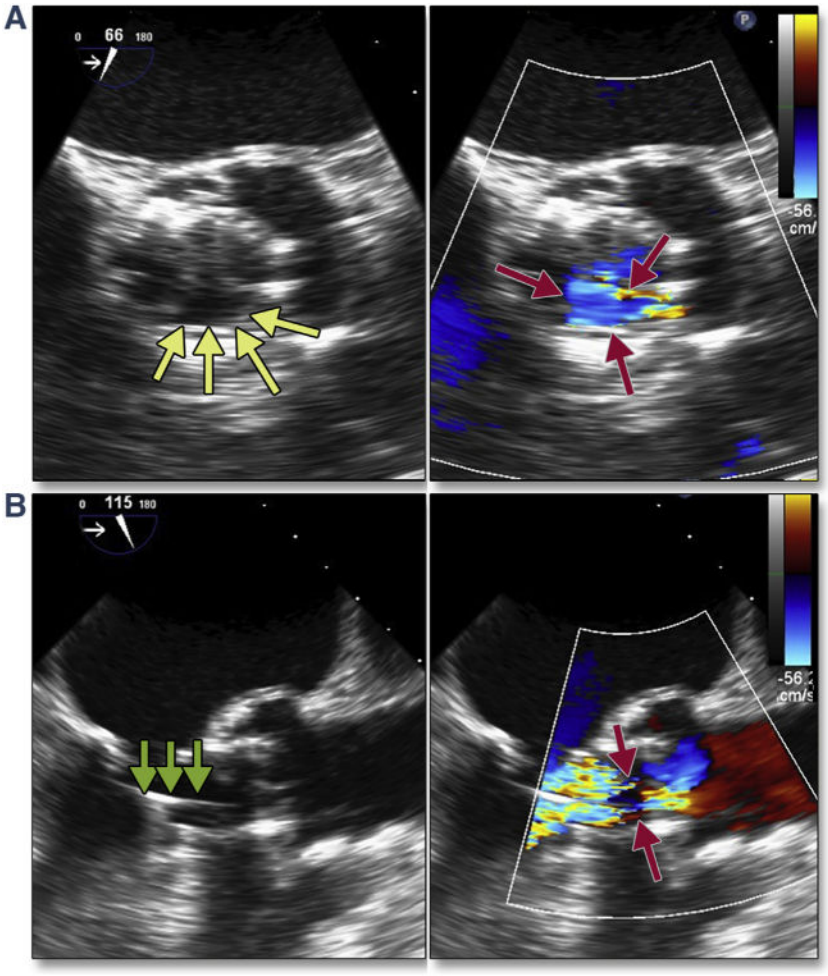

Figure 21. Severe Central Aortic Regurgitation

In these color compare images a transcatheter valve leaflet has been pinned open **(A, yellow arrows)** (Online Video 22) resulting in severe central aortic regurgitation (A and B, red arrows). This may be due to the stiff wire **(B, green arrows)**, which can respond to removal or manipulation of the wire.

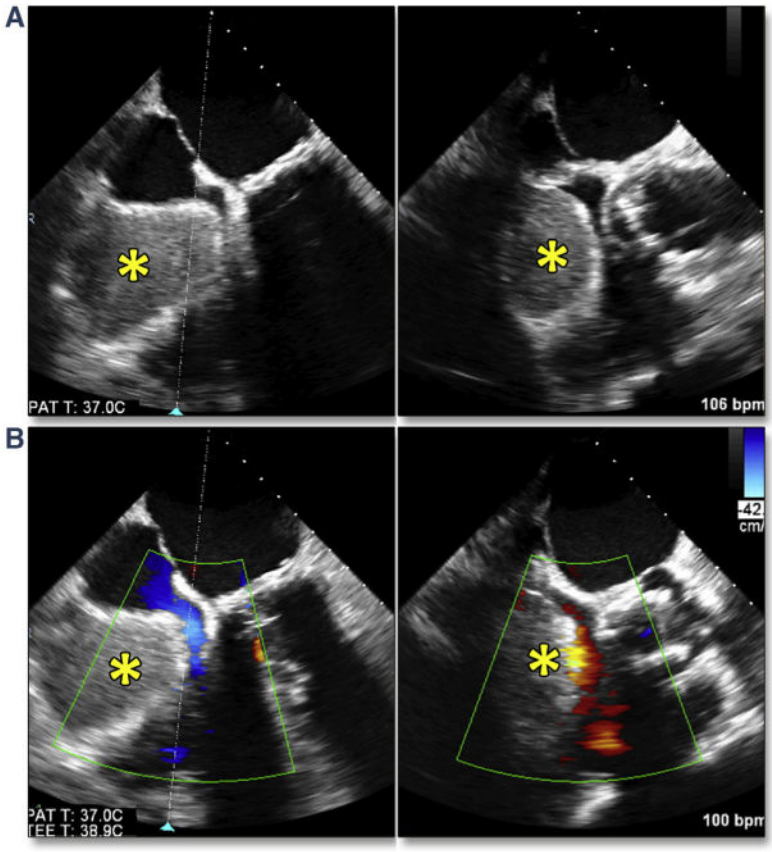

Figure 22. Acute Right Ventricular Perforation

After successful TAVR with no evidence of conduction abnormalities, the pacing wire was removed with immediate accumulation of blood seen by simultaneous multiplane imaging within the pericardial space **(A)** (Online Video 23) adjacent to the right ventricle **(*)**. This resulted in obstruction to the tricuspid valve flow **(B)** (Online Video 24) and ensuing tamponade physiology. Abbreviation as in Figure 5.

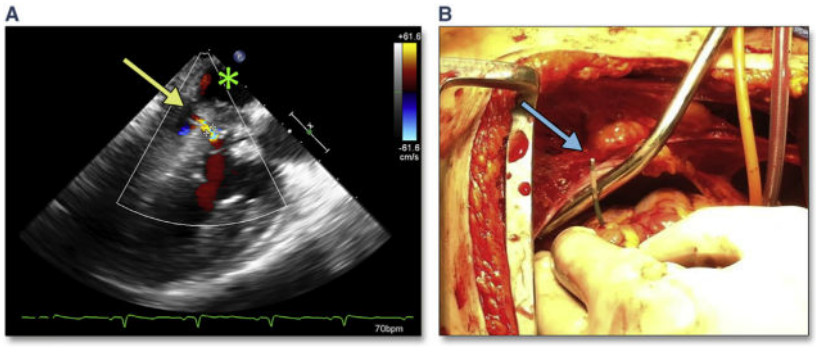

Figure 23. Ventricular Perforation

(A) A small, undetected left ventricular perforation occurred in the setting of a transaortic TAVR. On follow-up imaging, a ventricular pseudoaneurysm was seen **(A)** with flow from the left ventricle **(yellow arrow)** to the pericardial space **(green asterisk)**. **(B)** An example of a BAV catheter **(blue arrow)** through the left ventricle at open repair. This complication occurred during cardiopulmonary resuscitation with chest compressions. Abbreviations as in Figures 2 and 5.

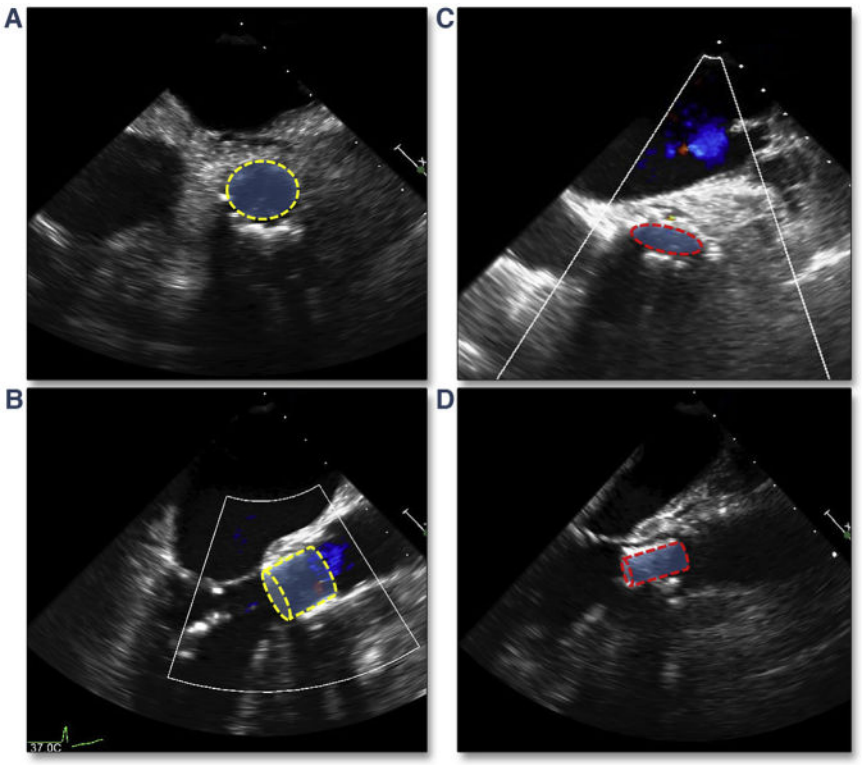

Figure 24. Crushed THV After CPR

(A) The short axis view, and **(B)** the long axis view after initial deployment of the THV. Chest compressions were subsequently necessary in the setting of an aortic rupture and short-axis **(C)** (Online Video 25) and long-axis **(D)** (Online Video 26) views show narrowing of the anterior-posterior dimension of the THV. Abbreviation as in Figure 8.

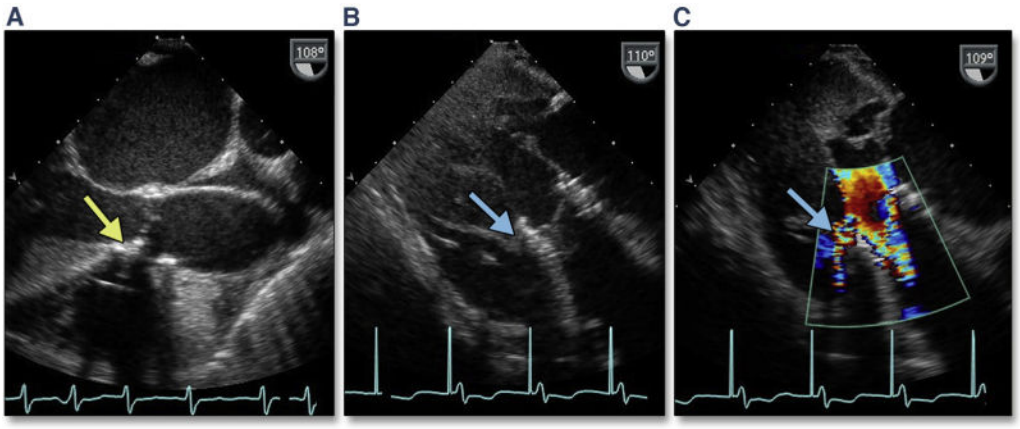

Figure 25. Ventricular Septal Rupture

Ectopic calcification may extend into the LVOT along the membranous septum **(A, yellow arrow)**. After TAVR, deep gastric long axis views may be the best views for imaging the defect in the membranous septum **(B, blue arrow)** (Online Video 27) with color Doppler **(C)** (Online Video 28) showing systolic flow across a traumatic ventricular septal defect. Abbreviations as in Figures 5 and 7.

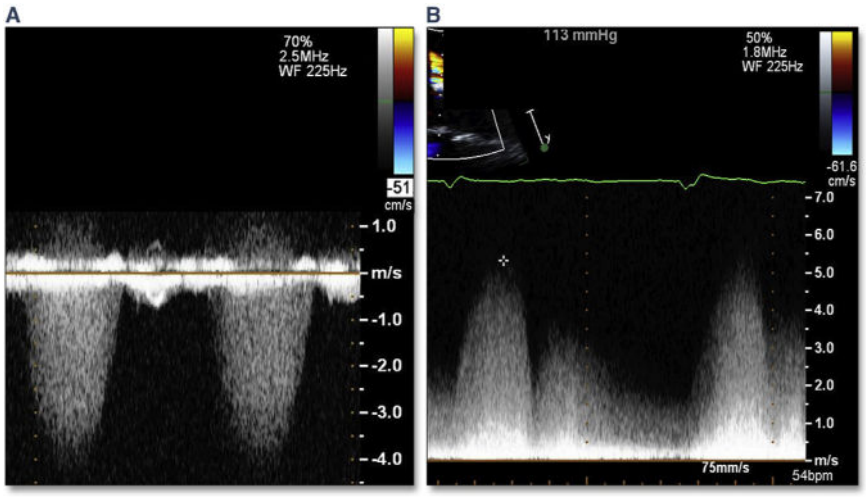

Figure 26. Atypical Doppler of Ventricular Septal Rupture From TAVR

(A) A typical continuous wave Doppler across a ventricular septal defect after TAVR. On follow-up transthoracic continuous wave Doppler **(B)**, there is prominent phasic but pan-cyclic flow representing aortic–to–right ventricular systolic and diastolic shunt. Abbreviation as in Figure 5.

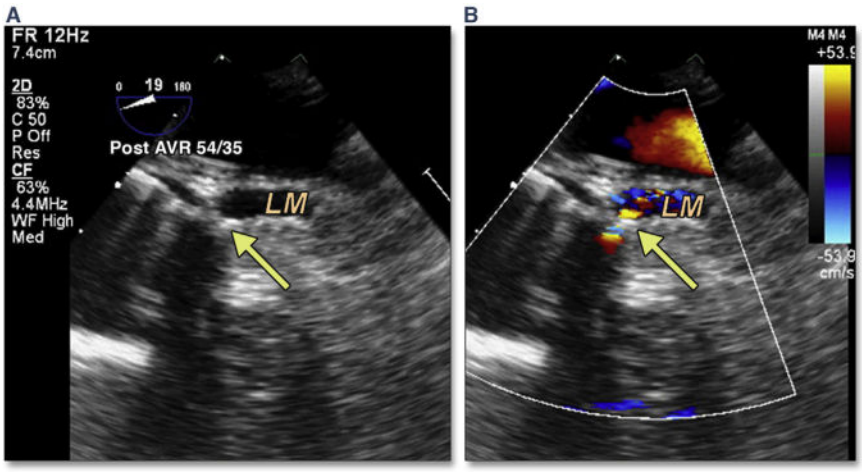

Figure 27. Coronary Occlusion

LM coronary occlusion can be imaged immediately after TAVR **(yellow arrow)** and is accompanied by acute left ventricular dysfunction and hemodynamic collapse (Online Video 29). Abbreviations as in Figures 4 and 5.

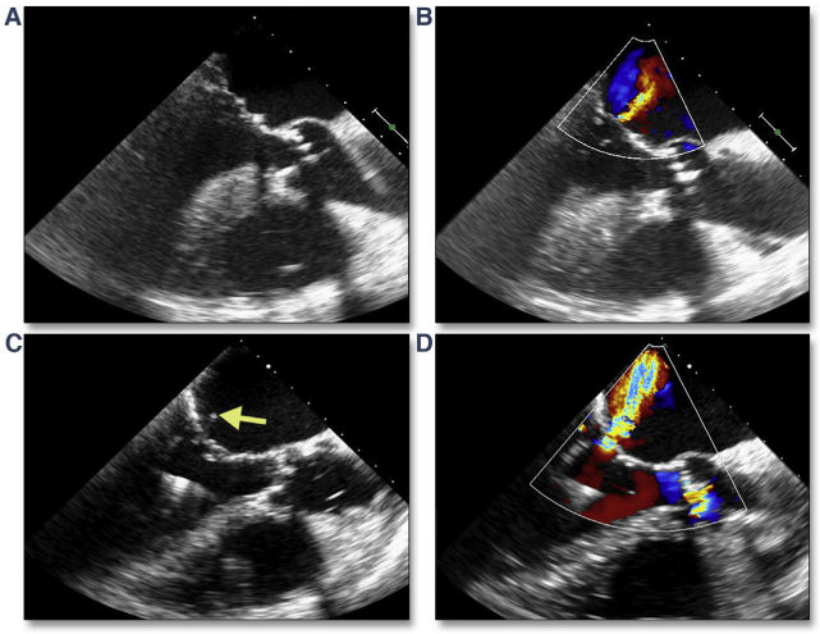

Figure 28. Acute Mitral Valve Regurgitation

At baseline, mitral chordae appear intact **(A)** (Online Video 30) with trace mitral regurgitation **(B)**. After stiff wire insertion and balloon aortic valvuloplasty, a ruptured mitral ruptured chordae **(C, yellow arrow)** (Online Video 31) results in moderate mitral regurgitation **(D)**.

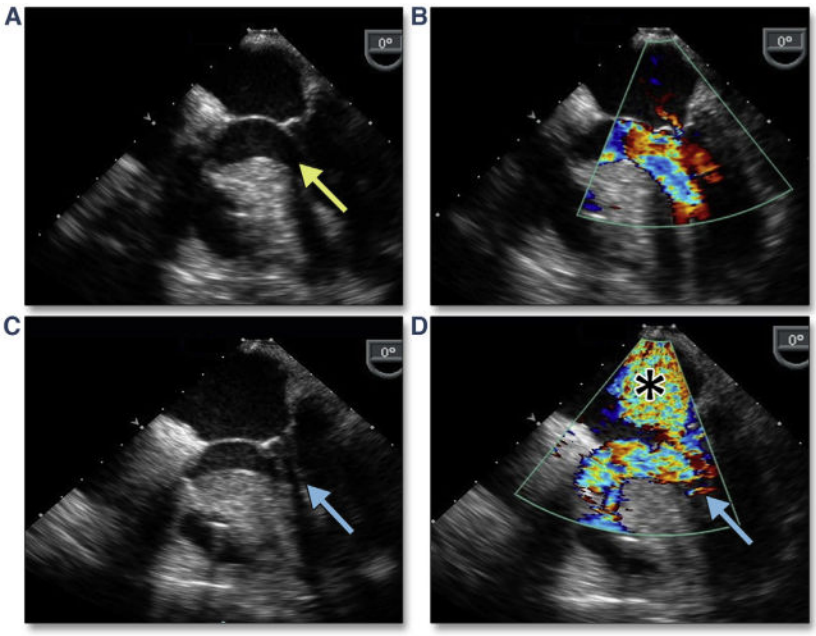

Figure 29. SAM of the Mitral Leaflet After TAVR

(A) A hypertrophied basal septum but without systolic anterior motion **(yellow arrow)** and no significant mitral regurgitation **(B)** (Online Video 32) before TAVR. After valve implantation, there is prominent systolic anterior motion (SAM) **(C, blue arrow)** with turbulent LVOT flow **(D, blue arrow)** (Online Video 33) and mitral regurgitation **(*)**. Abbreviations as in Figures 4 and 7.

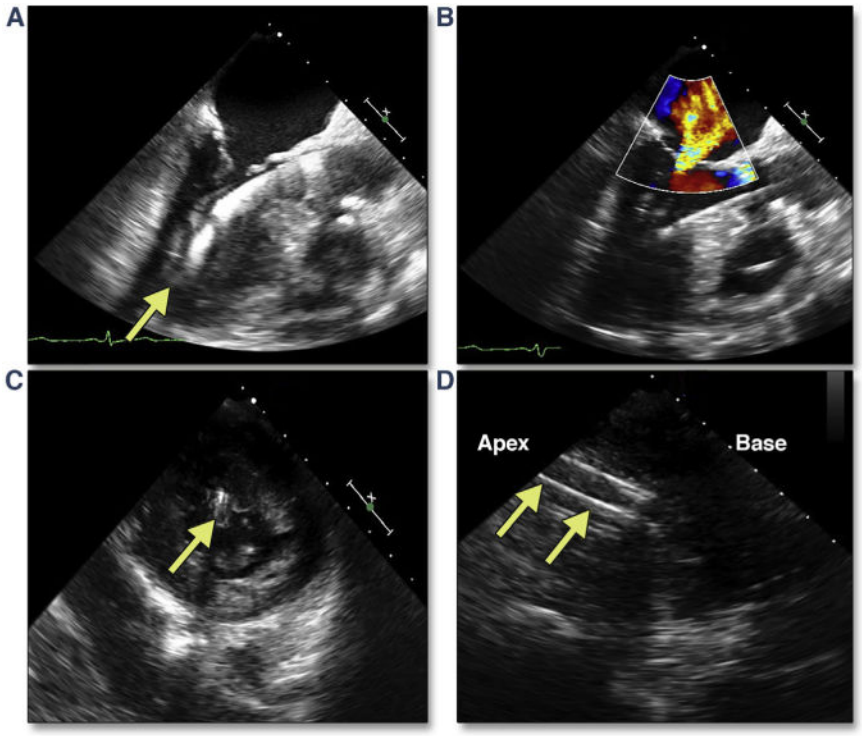

Figure 30. Papillary Muscle Transection Secondary to Transapical Cannulation

(A) The transapical cannula in a slightly posterior position (Online Video 34), with associated new-onset severe mitral regurgitation **(B)**. Deep gastric short axis **(C)** (Online Video 35) and long-axis **(D)** views of the left ventricle (LV) confirm that the cannula has passed through the posteromedial papillary muscle head **(yellow arrows)**.

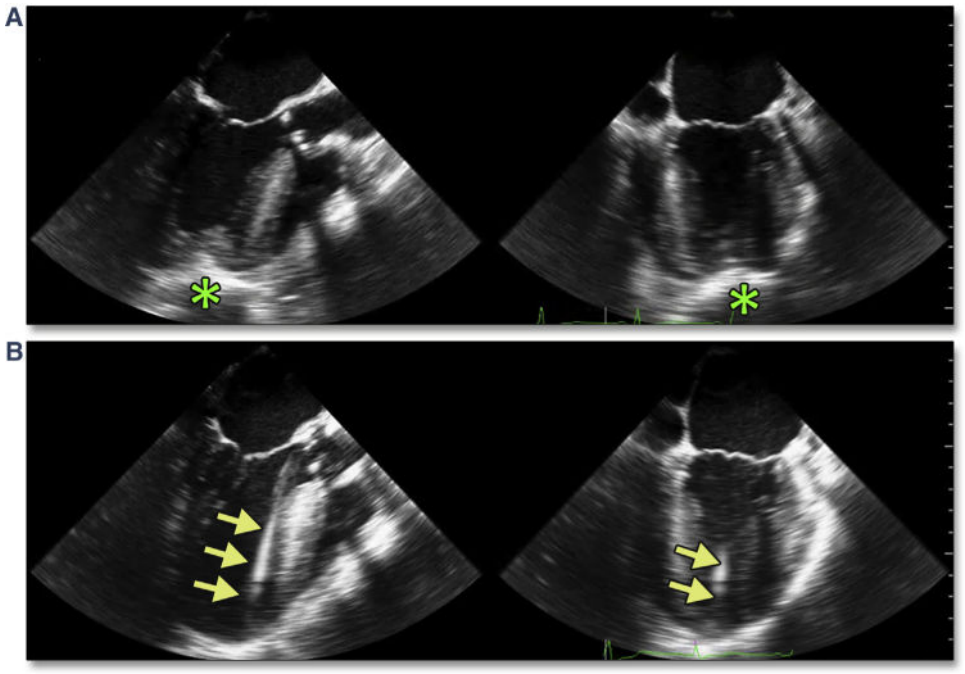

Figure 31. Confirmation of Apical Cannulation Site

After limited thoracotomy, the surgeon indicates the intended site of cannulation with an apical poke, which is easily identified in 2 orthogonal views with simultaneous multiplane imaging (**A** [Online Video 36]). When appropriately identified, wires pass freely into the LV and across the AV (**B** [Online Video 37]). Abbreviation as in Figures 18 and 30.

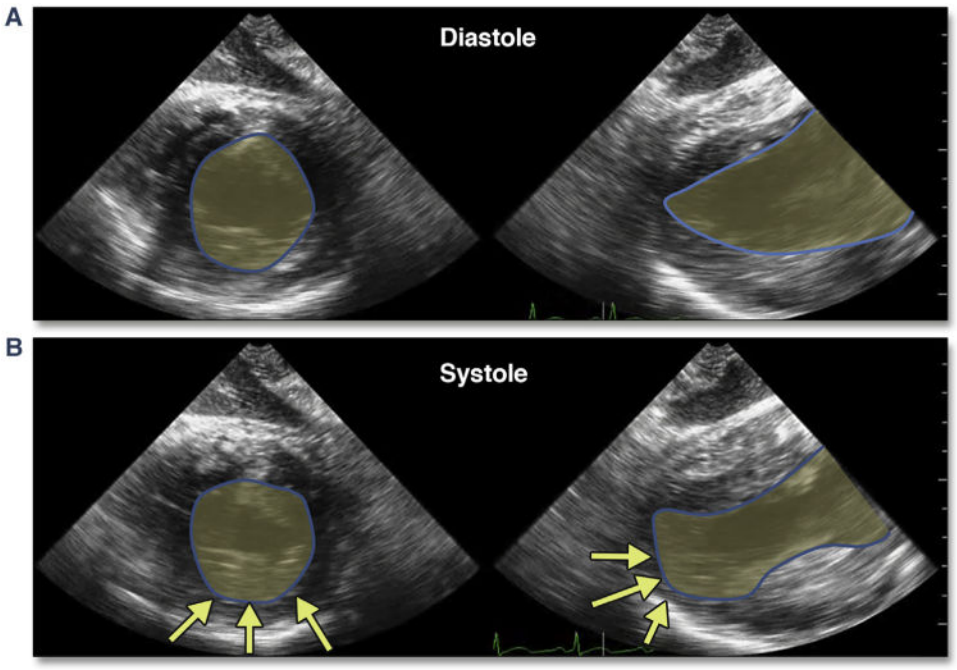

Figure 32. Indirect Obstruction of Distal Coronary Flow After Cannula Removal and Apical Closure Due to Tension From the Purse-String Sutures

Marked apical hypokinesis involving more than the immediate cannulation site is shown in this diastolic **(A)** and systolic **(B)** (Online Video 38) multiplane (Online Video 38, short-axis and long-axis) deep gastric views of the LV. Abbreviation as in Figure 30.

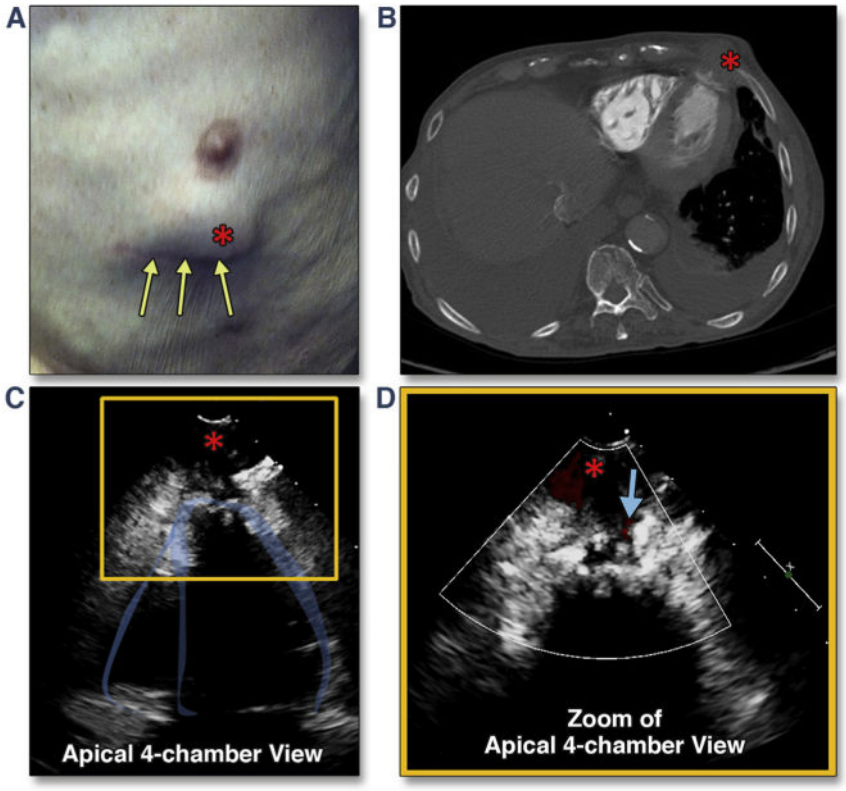

Figure 33. Apical Pseudoaneurysm Formation After Transapical Cannulation

This patient complained of an expanding chest wall mass **(A, red asterisk)** 6 months after transapical TAVR (**yellow arrows** show the mini-thoracotomy scar). Transthoracic imaging revealed a pseudoaneurysm, best seen from the apical views **(C, red asterisk)** (Online Video 39) with systolic flow detected on color Doppler **(D, blue arrow)** (Online Video 40). The finding was confirmed by both echocardiographic intravenous contrast study as well as chest computed tomography (CT) **(B)**. Abbreviation as in Figure 5.

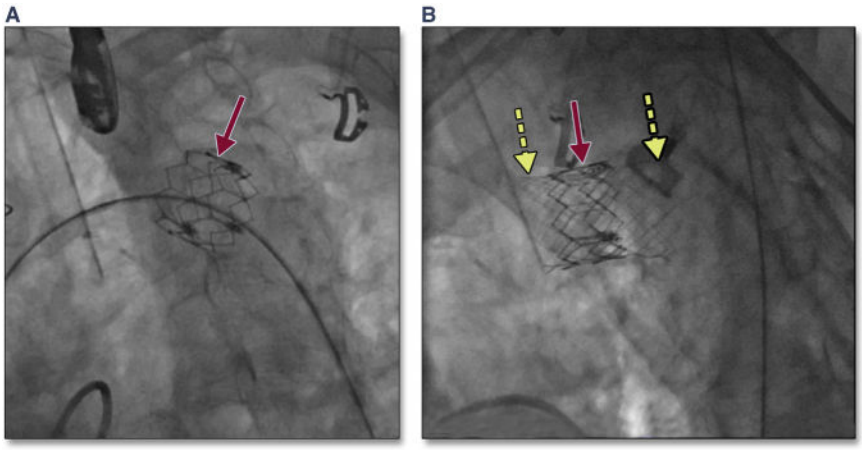

Figure 34. Distal Migration of the THV

Migration of the THV into the aortic arch **(A, red arrow)** may occur with high positioning of the THV. In this patient, with placement of a covered stent **(B, yellow dashed arrows)** was performed to exclude the valve component of the THV. Abbreviation as in Figure 8.

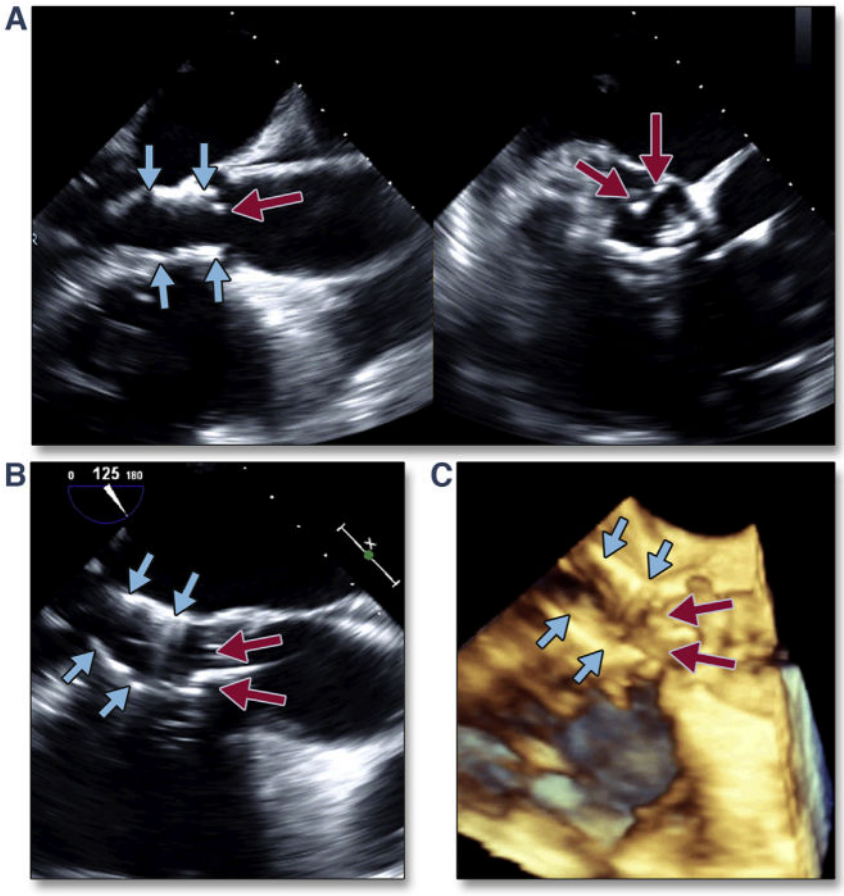

Figure 35. Translocation of the THV into the Ventricle

Migration of the THV into the LV can occur when the initial position of the valve is too low. The simultaneous multiplane image **(A)** (Online Video 41), with the long-axis view of the transcatheter valve on the left and the short-axis view on the right, shows the low position of the transcatheter valve **(blue arrows)** with significant native leaflet overhang **(red arrows)**. Translocation of the transcatheter valve is seen by both 2-dimensional **(B)** and 3-dimensional **(C)** (Online Video 42) imaging. Abbreviations as in Figures 8 and 30.

Table 1
Intraprocedural Complications Reported in the PARTNER Database (N = 527)

Failure to implant: **a.** Secondary to superior motion of balloon during BAV in setting of large sigmoid septum	1 (0.2%)
Balloon aortic valvuloplasty complications **a.** Severe aortic regurgitation: stuck or avulsed valve **b.** Aortic trauma	3 (0.6%)
Acute hemodynamic compromise **a.** LV collapse (expired) **b.** RV standstill (expired)	Left ventricle = 5 (1%) Right ventricle = 1 (0.2%)
Malposition **a.** Requiring surgical bailout (too low) or valve-in-valve procedure **b.** Embolization: **i.** Into aorta: due to loss of pacing capture (n = 1) **ii.** Into left ventricle (n = 1)	Surgical bail-out = 2 (0.4%) Valve-in-valve = 2 (0.4%)
Aortic complications **a.** Aortic dissection (proximal) caused by embolization of first valve **b.** Aortic annular rupture **c.** Descending aortic rupture **d.** Periaortic hematoma **i.** With RCA compression **ii.** With no hemodynamic consequence	Dissection 2 (0.4%) Annular rupture = 3 (0.6%) Periaortic hematoma = 3 (0.6%) Descending aorta rupture = 1 (0.2%)
Significant aortic regurgitation **a.** Severe central AR **i.** Pst-BAV **ii.** Post-THV (malposition, stuck cusp) **b.** Severe paravalvular AR **i.** Treated with post-dilation **ii.** Treated with valve-in-valve procedure (n = 5)	Severe central AR in THV = 2 (0.4%) BAV complication = 3 (0.6%) Valve-in-valve procedure = 5 (1%)
Bleeding/pericardial effusion **a.** Post transapical TAVR **i.** At cannulation site **ii.** Adjacent to cannulation site **iii.** Hemorrhagic pleural effusion (requiring pleurodesis) **b.** Pacemaker perforation **c.** LV or RV tear **d.** Post-BAV after chest compressions	Apical bleeding = 2 (0.4%) RV cannulated = 1 (0.2%) Pacemaker = 2 (0.4%) LV perforation = 3 (0.6%) BAV CPR = 1 (0.2%)
Fistulas	3 (0.6%)

a. Aorta-to-right atrium fistula	
b. Membranous VSD	
Coronary occlusion	3 (0.6%)
a. RCA (due to periaortic hematoma)	
b. Left main occlusion	
c. Post-transapical cannulation (distal LAD)	
Mitral valve regurgitation (acute)	1 (0.2%)
a. Mitral valve cusp perforation	
b. Wire entanglement	
Total	49 (9.3%)

Values are n (%).

AR = aortic regurgitation; BAV = balloon aortic valvuloplasty; CPR = cardiopulmonary resuscitation; LAD = left anterior descending coronary artery; LV = left ventricular; PARTNER = Placement of Aortic Transcatheter Valves; RCA = right coronary artery; RV = right ventricular; TAVR = transcatheter aortic valve replacement; THV = transcatheter heart valve; VSD = ventricular septal defect.

Table 2
Summary of Echocardiographic Imaging Recommendations

	Complication	Imaging Recommendations	
Wire position	Entanglement in mitral apparatus or ventricular perforation	**1**	2DE and particularly 3DE imaging of wire position
		2	Imaging of mitral valve: change in severity of mitral regurgitation or chordal disruption
		3	Exclude new pericardial effusion or shunt
BAV	Coronary occlusion Severe aortic regurgitation Aortic trauma	**1**	Image during and immediately after BAV for aortic leaflet motion and aortic regurgitation
		2	Image the coronary arteries (particularly the left main) for obstruction by the calcified leaflets
		3	Image the location of the displaced calcified leaflets for possible deformation of the aortic wall or annulus
Pacing or at any time during procedure	Acute hemodynamic collapse	**1**	Exclude acute valvular regurgitation
		2	Exclude aortic root trauma
		3	Exclude acute ventricular dysfunction
		4	Exclude coronary obstruction
		5	Exclude pericardial effusion/tamponade
Positioning of transcatheter valve	Malpositioning	**1**	Three different positions should be imaged typically from the mid-esophageal long axis view: during native beats, during pacing, and after final deployment
		2	During nonpaced beats, the diastolic valve position is ∼50% above and below the annulus. In the setting of normal ventricular function, the valve is typically higher in systole and should approximate the paced beat position
		3	During paced beats the valve should be 30% to 40% (∼5 to 6 mm) below the annulus
		4	Optimal final position is 10% to 20% (or 2 to 3 mm) below the annulus
		5	Superior or aortic edge of the stented valve should be imaged; the native calcified cusps must be covered by 1 to 2 mm while remaining inferior to the sinotubular junction
Transapical cannulation	Cannulation site misplacement	**1**	Confirm location of the transapical puncture site by imaging the apex (either from mid-esophageal views or transgastric views)
		2	The site should avoid the right ventricle and be angulated away from the interventricular septum
		3	Assess post-TAVR apical wall motion and exclude persistent transapical flow
Deployment	Aortic dissection or periaortic hematoma	**1**	Estimate risk of aortic trauma with evaluation of calcium within the left ventricular outflow tract, sinuses, and sinotubular junction
		2	Watch location of displaced calcium during BAV and during valve deployment
	Paravalvular aortic regurgitation	**1**	Appropriately size the THV with 3DE measurement of the annulus

Complication	Imaging Recommendations	
	2	Estimate risk of paravalvular regurgitation with evaluation of calcium within the LVOT and annulus
	3	Assess likelihood for effective post-dilation (less effective with severe LVOT calcium)
	4	Assess risk of post-dilation (i.e., left main occlusion or annular/aortic rupture)
Coronary occlusion	**1**	Estimate risk of coronary occlusion with 3DE measurement of left coronary artery height and left coronary cusp length
	2	Estimate risk of coronary occlusion by observing the left main orifice and displacement of calcium during BAV
Acute LVOT obstruction	**1**	Assess risk (i.e., small, hypertrophied LV, narrow LVOT, septal hypertrophy)

2DE = 2-dimensional echocardiography; 3DE = 3-dimensional echocardiography; LVOT = left ventricular outflow tract; other abbreviations as in Table 1.